Nanostructures Technology, Research and Applications

Academic and Research Staff
Prof. Karl Berggren, Dr. Rajesh Menon, Mark. K. Mondol, Dr. Euclid Moon Dr. Mark L. Schattenburg, Prof. Henry I. Smith

Visiting Scientists, Postdoctoral Associates and Research Affiliates
Dai-Hyun Kim, Dr. Kristine Rosfjord, Dr. Timothy Savas, Dr. Michael Walsh, Dr. Feng Zhang

Graduate Students
Vikas Anant, Will Arora, Bryan Cord, Eric Dauler, Stefan Harrer, Charles Holzwarth, Xiaolong Hu, Jan Kupec, Joshua Leu, Anthony Nichols, Tom O'Reilly, Amil Patel, Hsin-Yu Tsai, Donald Winston, Joel Yang

Collaborators
Prof. Mark Baldo, Prof. George Barbastathis, Prof. Vladimir Bulovic, Dr. Fernando Castano, Prof. Jesus DelAlamo, Prof. Judy Hoyt, Prof. Erich Ippen, Prof. John Kasakian, Prof. Franz Kaertner, Prof. Leslie Kolodziejski, Prof. Jing Kong, Dr. Jagadeesh Moodera, Prof. Rajeev Ram, Prof. Caroline Ross, Prof. Edwin L. Thomas, Prof. Carl Thompson

Technical and Support Staff
James Daley, Tiffany Kuhn

1. Nanostructures Laboratory

The NanoStructures Laboratory (NSL) at MIT develops techniques for fabricating surface structures with feature sizes in the range from nanometers to micrometers, and uses these structures in a variety of research projects. The NSL is closely coupled to the Space Nanotechnology Laboratory (SNL) with which it shares facilities. The NSL and SNL include facilities for lithography (photo, interferometric, electron-beam, imprint, and x-ray), etching (chemical, plasma and reactive-ion), liftoff, electroplating, sputter deposition, and e-beam evaporation. Much of the equipment, and nearly all of the methods, utilized in the NSL/SNL are developed in house. Generally, commercial lithography and processing equipment, designed for the semiconductor industry, cannot achieve the resolution needed for nanofabrication, is inordinately expensive, and lacks the required flexibility for our research. This report does not cover all of the research conducted in the NSL facilities, but instead focuses on those that support advance the state of the art of nanofabrication and others under Prof. Henry I. Smith.

2. Scanning-Electron-Beam Lithography (SEBL) Facility

Sponsors:
MIT Institute facility under RLE

Project Staff:
Mark K. Mondol, Dr. Feng Zhang, Prof. Henry I. Smith, Prof. Karl Berggren

In 2004, the Nanostructures Lab converted its scanning-electron-beam-lithography (SEBL) facility in Room 38-165 into an Institute-wide service facility under the Research Laboratory of Electronics (RLE). This facility provides MIT and outside users with easily accessible e-beam lithography, coupled with resident expertise and advice. The facility is managed by Mark Mondol who provides training on the e-beam tools, direct patterning service, and advice on optimal nanofabrication techniques and strategies. The NanoStructures Laboratory (NSL) and the

Microsystems Technology Laboratories (MTL) have service facilities for spin coating of resists, resist development and other forms of processing.

Projects that made use of the SEBL facility during the past year included: patterned nanotube growth; relief templates for self assembly of block copolymers; point-contact devices; 1-D and 2-D photonic crystals; ring-resonator add/drop filters; optical-polarization splitter-rotator devices; novel liquid-crystal devices; magnetic-memory devices; quantum photodetectors; templates for nanoimprint lithography; photomasks for interferometric-spatial-phase-imaging alignment and gapping; 4-point contacts for measurements on nanotubes and nanowires; III-V compound T-gate HEMTs and arrays of Fresnel zone plates. Research in lithographic processing included extreme cold development of PMMA and novel developer solutions for HSQ which demonstrated improved resolution and contrast. Use of the facility, by the MIT community, was widespread, there were: 25 Principal Investigators, 7 Departments, 8 Labs or Centers, 2 non-MIT entities and 45 distinct trained users over the last year.

Two SEBL tools are available. The Raith Turnkey 150 system is shown in Figure 1. Its electron-optical column is essentially identical to that of a Zeiss Gemini SEM, and provides a beam diameter as fine as 2 nm. Linewidths of ≤ 9 nm have been written with the system, as illustrated in Figure 2. The Raith 150 includes a pattern generator and laser-interferometer-controlled stage with an integrated software package which was upgraded to version 4.0 in the past year. This upgrade improved writing speed and system stability. Version 4.0 software now allows users to do automated field alignment to approximately ± 25nm. The system can operate from 1 to 30keV accelerating voltage. Wafers up to 150 mm can be loaded into the system. Typically, users are trained for 3 to 10 hours and then allowed to operate the tool on their own. The tool is available, for most users, 24 hours a day, 7 days a week.

Figure 3 is a photograph of the VS-26 system. This instrument was put together at MIT from two systems (VS-2A and VS-6) obtained as gifts from IBM in the mid 1990's. VS-26 has a minimum beam diameter of about 10 nm. It operates at a fixed accelerating voltage of 50keV. Conversion software has been developed which allows a CAD data file to be fractured and translated prior to exposure, additional software was developed to generate arbitrary arcs. Substrates up to 200 mm diameter can be exposed at linewidths down to ~30 nm. However, the area available for patterning is limited to 95x95 mm.

The Raith 150 is used in a program to develop spatial-phase-locked e-beam lithography, described elsewhere. The objectives of that program are to achieve sub-1 nm pattern-placement accuracy, and to reduce the cost and complexity of SEBL. In a conventional SEBL system costing several million dollars, pattern placement accuracy is typically much worse than 10 nm.

The SEBL facility encourages users with a variety of experience levels and requirements. Experienced users are able to carry out complex, multilevel aligned exposures on the Raith-150 tool. Less experienced users get hands-on instructions from facility staff, and guidance during the learning and initial fabrication stages.

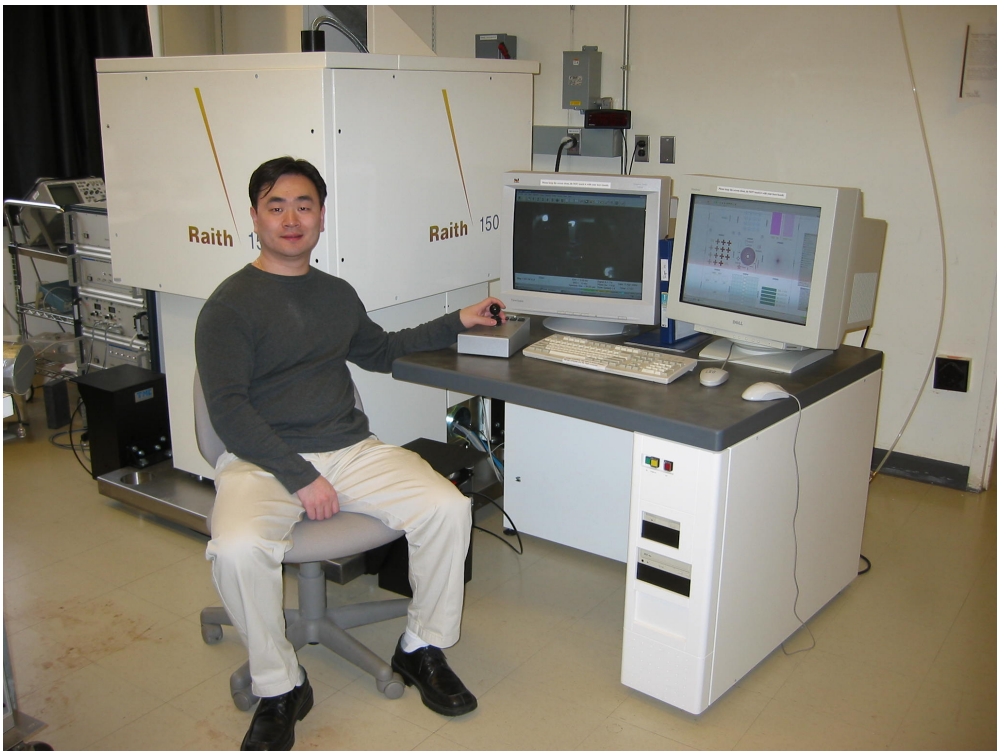

Figure 1. *The Raith-150 electron-beam lithography system. This tool provides sub-20-nm patterning resolution, and pattern-placement accuracy ~ 1nm via spatial phase locking. The operator is Dr. Feng Zhang.*

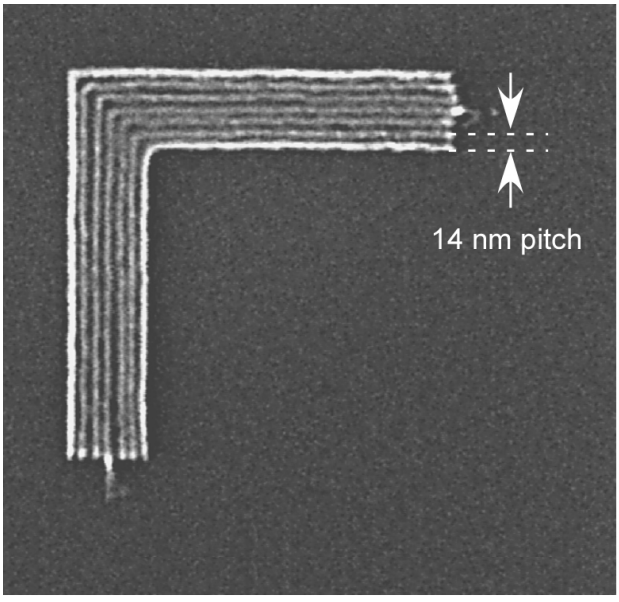

Figure 2: *Scanning-electron micrograph of exposed and developed HSQ illustrating the resolution of the Raith 150 SEBL system. (J. K. W. Yang and K. K. Berggren, "Using High-Contrast Salty Development of Hydrogen Silsesquioxane for Sub-10-nm-Half-Pitch Lithography," Journal of Vacuum Science & Technology B, submitted for publication (2007))*

.

Figure 3. *Photograph of the VS-26 scanning-electron-beam lithography system.*

3. Spatial-Phase-Locked Electron-Beam Lithography

Sponsors
National Science Foundation

Project Staff
Dr. Euclid E. Moon, Prof. Henry I. Smith, Prof. J. Todd Hastings (U. Kentucky)

Our research in spatial-phase-locked electron-beam lithography (SPLEBL) is conducted in collaboration with the University of Kentucky. It is aimed at reducing pattern-placement errors in electron-beam-lithography systems to the sub-1 nm level. Such high precision is essential for certain applications in photonics and nanoscale science and engineering. SPLEBL is currently the only approach capable of achieving such pattern-placement accuracy. As shown in Fig. 1, SPLEBL uses a periodic signal, derived from the interaction of the scanning e-beam with a fiducial grid placed directly on the substrate, to continuously track the position of the beam while patterns are being written. Any deviation of the beam from its intended location on the substrate is sensed, and corrections are fed back to the beam-control electronics to cancel beam-position errors. In this manner, the locations of patterns are directly registered to the fiducial grid on the substrate.

The research effort at MIT is now focused on developing the materials and processes for producing the fiducial grid, with the objectives of: maximizing the signal-to-noise of the secondary-electron signal derived from the grid; minimizing electron scattering from the grid, which would be deleterious to precision lithography; maximizing the area and absolute accuracy of the grid; and minimizing the cost and inconvenience of producing the grid on substrates of interest. We have determined that signal levels are maximized when the grid is formed from nanoparticles. Substrates have been patterned with in-situ Faraday cups, as illustrated in Fig. 2, to make accurate measurements of signal-to-noise for a wide variety of nanoparticle types. To minimize electron scattering, the nanoparticles must be composed of low-atomic-number materials. Fullerenes may be the optimal nanoparticle, but achieving uniform thickness of layers and attaching the fullerenes along the grid lines represents a challenge of attachment chemistry. Scanning-beam interference lithography will be used to produce master grids. A special form of imprint lithography that maintains long-range spatial-phase coherence will be used to transfer attachment-chemistry grid patterns onto substrates of interest. The research effort at the University of Kentucky is focused on processing of the signal from the grid. Previous approaches utilized only the raster-scan mode. New approaches are being developed that enable spatial-phase locking while e-beam writing is conducted in a vector-scan mode.

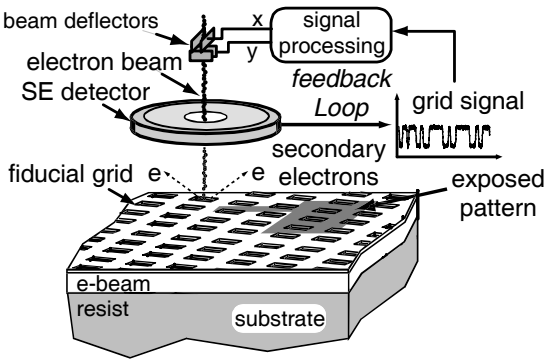

***Figure 1**: Schematic of the global-fiducial-grid mode of spatial-phase-locked electron-beam lithography. The periodic signal detected from the fiducial grid, which includes both X and Y components, is used to measure placement error, and a correction signal is fed back to the beam deflection system.*

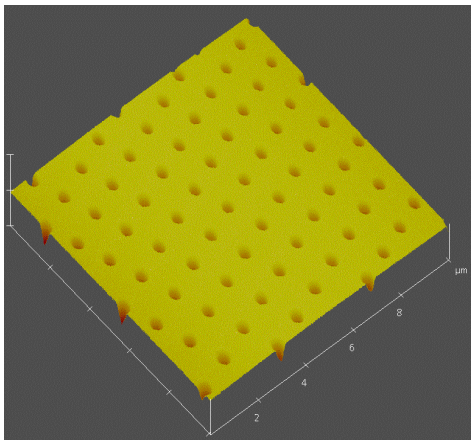

***Figure 2**: AFM scan of in-situ Faraday cups used to measure signal-to-noise for a variety of nanoparticles forming fiducial grids.*

References

[1] J.T. Hastings, F. Zhang, and H.I. Smith, "Nanometer-level stitching in raster-scanning e-beam lithography using spatial-phase locking," *J. Vac. Sci. Technol.* B, **21**, 2650 (2003).

[2] F. Zhang, H.I. Smith and J.F. Dai, "Fabrication of high-secondary-electron-yield grids for spatial-phase-locked electron-beam lithography," *J. Vac. Sci. Technol.* B, **23**, 3061 (2005).

4. Imprint Lithography

Sponsors:
AFOSR

Project Staff:
Dr. Euclid E. Moon, Prof. Karl K. Berggren, Prof. Henry I. Smith

Imprint lithography is a straightforward and reliable means of replicating patterns from a template with feature sizes below 10 nm. Experiments have also demonstrated replication of features at the single-molecule level. Typically, the imprint template consists of a thick, fused-silica blank coated with 100 nm of hydrogen silsesquioxane (HSQ), patterned by scanning-electron-beam lithography (SEBL). The patterned template is treated with a release-assist agent such as alkyltrichlorosilane, which reduces the surface free energy of the template, and ensures that the template can be removed cleanly after imprint. A planarization layer material is spun on a silicon wafer, followed by nanoliter droplets of a low-viscosity etch-barrier fluid. The template is leveled and brought into proximity with the substrate. Upon contact, the etch barrier fluid distributes itself by capillary action throughout the cavities in the template pattern. Low pressure is applied to the template, slightly compressing the etch barrier fluid, and allowing a three-point force measurement around the periphery of the template to ensure proper leveling. The gap between the template and substrate is maintained at ~100 nm, which allows freedom of movement of the template parallel to the substrate, with the etch barrier fluid acting as a lubricating layer. Alignment is performed to the ~1-nm level using our novel Interferometric-Spatial-Phase Imaging (ISPI) alignment technology. A brief exposure of the etch barrier fluid to ultraviolet light initiates crosslinking of monomers in the fluid, after which the template is removed in a measured and level manner. The pattern remaining in the solidified etch barrier material is transferred into the substrate with a bi-layer reactive-ion etch.

Two custom-designed imprint lithography systems are in the NanoStructures Laboratory (NSL), one of which is illustrated in Fig. 1. The system can imprint on wafers up to 200 mm diameter, in field sizes up to 25 x 25 mm. Stage position is feedback-controlled in X, Y, and Z to ~1 nm. Template leveling is controlled at three points to ~1 nm. Alignment and gap are detected simultaneously with a set of three ISPI microscopes. Both imprint systems reside in micro-environment enclosures within a Class 10 cleanroom.

Exploration of synergy between imprint lithography and Zone-Plate-Array Lithography (ZPAL), Interferometric Lithography (IL), Spatial-Phase-Locked E-Beam Lithography (SPLEBL), and other types of nanolithography unique to the NSL are underway. In an example of such synergy, the high-throughput, parallel-write capabilities of ZPAL are being used to streamline patterning of imprint templates. In another example, imprint lithography is being used to inexpensively transfer IL-patterned fiducial grids onto substrates, a step that may be essential to successful commercialization of SPLEBL. In yet another example (illustrated in a subsequent section), we use imprint lithography to fabricate arrays of zone plates.

We plan to employ imprint lithography systems for fabrication of coupled Josephson junction quantum bits for use in quantum computing.

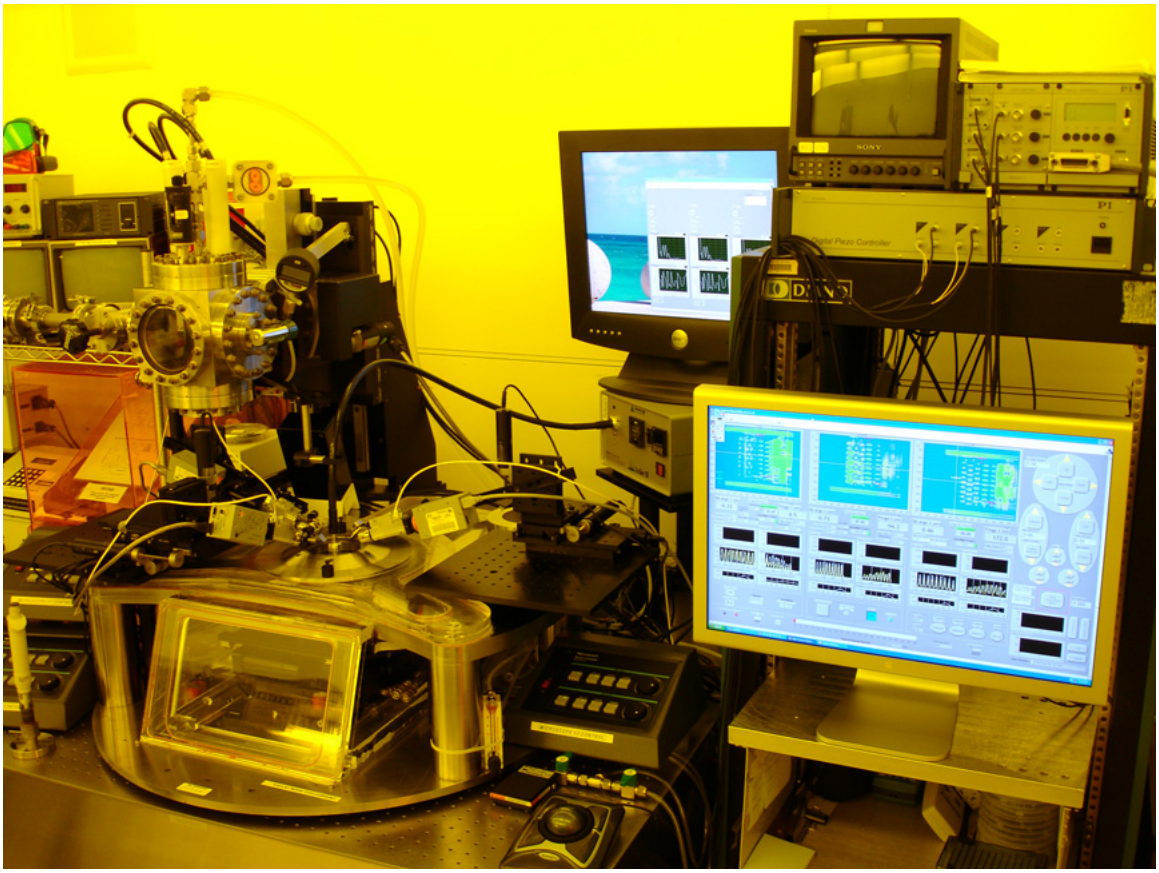

Figure 1: A custom-designed imprint lithography system used with Interferometric-Spatial-Phase Imaging (ISPI) alignment and gap control. Three ISPI microscopes provide continuous position measurements for six-axis positioning (X, Y, Z, θ_x, θ_y, θ_z) with sub-1 nm precision.

5. Imprint Lithography with Multilevel Alignment Via Interferometric-Spatial-Phase Imaging

Sponsors
Internal funds

Project Staff
Dr. Euclid E. Moon, Prof. Henry I. Smith

A critical requirement for widespread industrial utilization of imprint lithography is multilevel overlay capability. In journal articles [1, 2] we described a position metrology scheme, called Interferometric-Spatial-Phase Imaging (ISPI), which encodes alignment in the spatial phase disparity of complementary interference fringes, observed with oblique-incidence, long-working-distance, darkfield optical microscopes. We have applied ISPI to step-and-flash imprint lithography (S-FIL), in which alignment is actively measured and corrected with imprint fluid filling the template-substrate gap.

In previous S-FIL work, alignment marks were placed entirely outside of the imprinted area. However, it is highly desirable to detect alignment within the imprinted region, which implies use of a shallow phase grating as the alignment mark, and raises the issue of ISPI fringe contrast. Fringe contrast with a fused silica phase grating in an imprint fluid is 12% of the fringe contrast

with air in the template-substrate gap, as predicted by two-dimensional finite-difference time-domain (FDTD) simulations, and confirmed by experiment. Despite the low fringe contrast, experimental data (Figure 1) shows that ISPI can achieve *sub-nanometer* alignment detectivity under such conditions, the most stringent typically encountered in imprint lithography.

Figure 2 illustrates dynamic alignment control throughout the S-FIL imprint process. The data shows an initial condition in which ISPI controls alignment to <1 nm. In this particular example, alignment is disturbed by a mechanical impulse from opening of the UV shutter, but such disturbances, which would usually pass unnoticed, can be observed and corrected by ISPI. We believe these experiments, among others, indicate that ISPI is uniquely suited for application to S-FIL and other forms of imprint lithography. Commercial S-FIL imprint lithography tools now incorporate ISPI alignment technology, and have demonstrated overlay of 3σ = 7 nm.

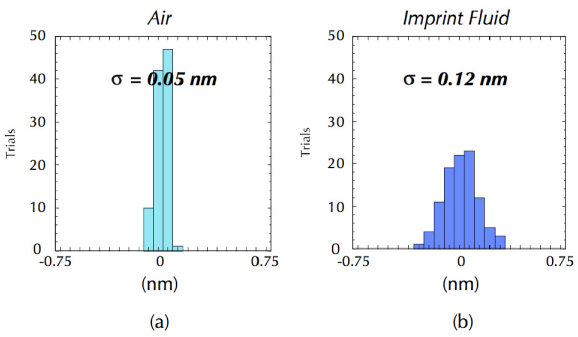

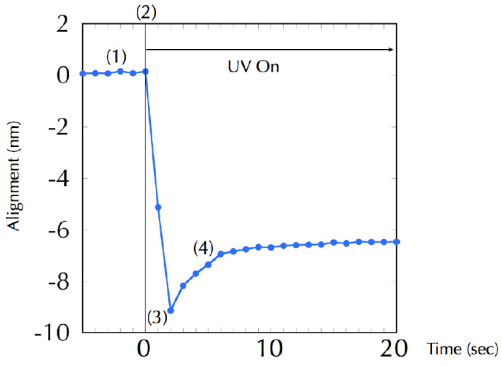

Figure 1: Alignment detectivity of ISPI with (a) air in the template-substrate gap (σ = 0.05 nm), and (b) imprint fluid in the gap (σ = 0.12 nm). Detectivity is reduced in the stringent case of phase gratings on the template, used with an imprint fluid of similar index of refraction, but remains within the sub-nanometer range. The template-substrate gap was mechanically locked during the experiment.

Figure 2: Plot of ISPI alignment data (1) before exposure, (2) at the instant the shutter to the UV lamp opens, (3) during misalignment caused by a mechanical shock transmitted from the UV lamp to the template, and (4) during correction of misalignment, until croslinking solidifies the imprint fluid. The experiment demonstrates the ability of ISPI to detect and identify sources of misalignment on the nanometer level, as well as a limited ability to re-align during crosslinking of the imprint material. Improvements are readily achievable with increased feedback bandwidth.

References

[1] E. E. Moon, L. Chen, P. N. Everett, M. K. Mondol, and H. I. Smith, "Interferometric-spatial-phase imaging for six-axis mask control," *J. Vac. Sci. Technol*. B **21**, 3112 (2003).

[2] E. E. Moon, M. K. Mondol, P. N. Everett, and H. I. Smith, "Dynamic alignment control for fluid-immersion lithographies using interferometric-spatial-phase imaging," *J. Vac. Sci. Technol*. B **23**, 2607 (2005).

6. Zone-Plate-Array Lithography (ZPAL)

Sponsors:
DARPA and NSF

Project Staff:
Dr. Rajesh Menon, Hsin-Yu Tsai and Prof. Henry I. Smith

Optical projection lithography (OPL) has been the key enabler of the continued improvements in performance of silicon integrated electronics. Modern OPL systems are designed for both high resolution and high-volume production. This has resulted in capital costs of tens of millions of dollars for OPL systems, putting them out of reach for applications other than high-volume production. Moreover, to achieve high resolution, various resolution-enhancement and proximity-effect-correction techniques must be employed. This, in turn, makes the cost of masks prohibitive for low-volume production and for research. To address this dilemma, the NanoStructures Lab has for several years been developing an entirely new approach to OPL, depicted in Fig. 1, called zone-plate-array lithography (ZPAL) [1]. No mask is required and writing is done in a dot-matrix fashion, which makes proximity-effect correction orders-of-magnitude simpler computationally.

In ZPAL the array of beamlets is created by an array of high-numerical aperture zone plates. The illumination of each zone plate is controlled by one pixel on an upstream spatial-light modulator. This technology is currently being commercialized by LumArray Inc. [2]. Figure 2 shows the roadmap for continued improvement in resolution.

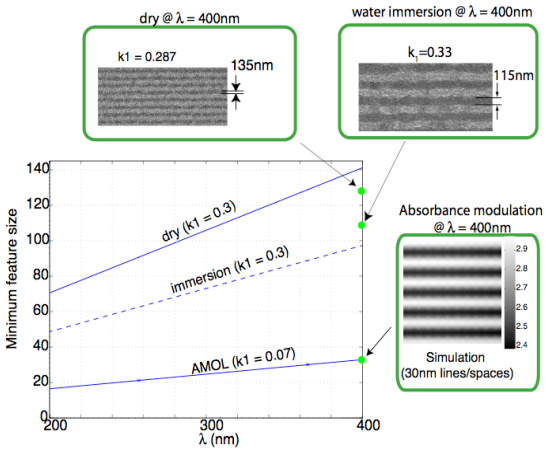

Figure 2: Roadmap for extending ZPAL to the 22 nm node. The micrographs show experimental results for λ = 400 nm. The side plot is a simulation of result expected with Absorbance Modulation Optical Lithogrpahy (AMOL) using existing photochromic materials. AMOL, is a recent invention at MIT [3,4] described elsewhere in this report.

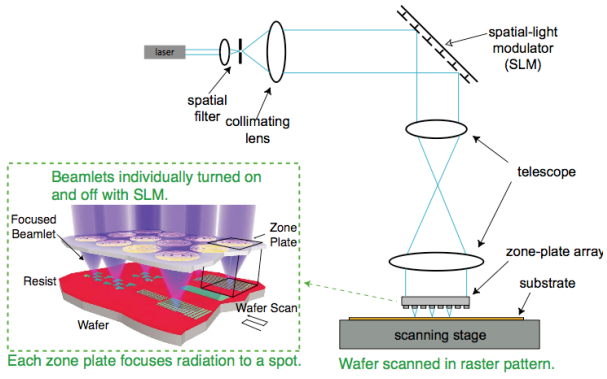

Figure 1: Schematic of zone-plate array lithography (ZPAL). Light from a CW laser illuminates a spatial-light modulator (SLM)which redirects the light to an array of phase zone plates. These, in turn, focus the light to diffraction-limited spots on axis, with 40% efficiency. Each pixel of the SLM addresses one zone plate of the array, and adjusts the intensity from zero to the maximum in a quasi-continuous manner. By moving the stage and adjusting the intensity of each focal spot under computer control, patterns of arbitrary geometry can be created in a dot-matrix fashion.

References
[1] H. I. Smith, R. Menon, A. Patel, D. Chao, M. Walsh, G. Barbastathis, "Zone-plate-array lithography: a low-cost complement or competitor to scanning-electron-beam lithography," Microelectronic Engineering, vol. 83, pp.956-961 (2006).
[2] www.lumarray.com

7. Absorbance-Modulation Optical Lithography (AMOL)

Sponsors:
DARPA and internal funds

Project Staff:
Rajesh Menon, Hsin-Yu Tsai, Prof. Henry I. Smith

We are investigating absorbance modulation as a means to overcome the diffraction limit in far-field, optical-projection imaging. A substrate is coated with an absorbance-modulation layer (AML) in which illumination at one wavelength, I_2, renders the AML opaque, while illumination at a shorter wavelength, I_1, renders it transparent. When illuminated with a ring-shaped spot at I_2 co-incident with a focused spot at I_1, the dynamic competition results in a nanoscale aperture, through which I_1 can penetrate to the substrate beneath (see Fig. 1). The size of the aperture is limited only by the photokinetic parameters of the AML, and the intensities of the illuminations [1].

If the AML is placed atop a photoresist that is sensitive to I_1 but not to I_2, patterns of arbitrary geometry can be written by scanning the substrate. The writing speed can be increases by using a large number of independently illuminated lenses operating in parallel, and scanning the stage [2]. This technology, which we call Absorbance-Modulation Optical Lithography (AMOL), will be maskless, fast, nanoscale and low-cost. AMOL resolution is determined by the ratio of the intensities at the two wavelengths. By simply scaling this ratio, it is possible to scale the transmitted spot far beyond the diffraction limit, enabling AMOL to eventually replace scanning-electron-beam lithography.

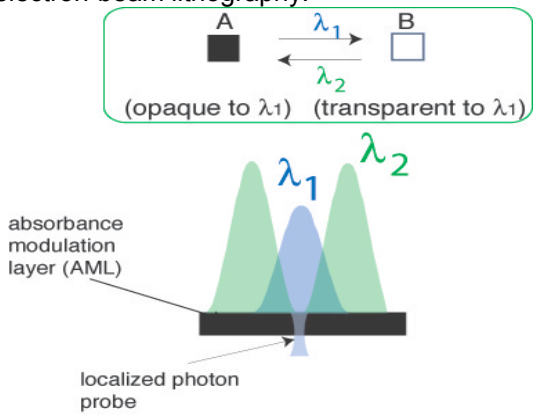

Figure 1: Absorbance modulation. The absorbance modulation layer can be made transparent or opaque depending upon the wavelength of illumination. By illuminating with both wavelengths at appropriate intensities, a stable, transparent aperture of nanoscale dimensions can be generated as shown.

References
[1] R. Menon and H. I. Smith, "Absorbance modulation optical lithography,"*J. Opt. Soc. Amer. A*, 23, 2290 (2006); R. Menon, H-Y Tsai and S. W. Thomas III, "Far-field generation of localized light fields using absorbance modulation," *Phys. Rev. Lett.* 98, 043905 (2007).

[2] H. I. Smith, R.Menon, A. Patel, D. Chao, M. Walsh, G. Barbastathis, Zone-plate-array lithography:a low-cost complement or competitor to scanning-electron-beam lithography," *Microelectron. Eng.*, 83, 956 (2006).

8. Replication of Diffractive-Optical Arrays Via Imprint Lithography

Sponsors
Internal funds

Project Staff
Dr. E. E. Moon, M. D. Galus, Dr. R. Menon, Prof. H. I. Smith

Diffractive-optical arrays serve important functions in a variety of applications, including zone-plate-array maskless lithography, in which they focus light to diffraction-limited spots and expose multiple features in parallel. Diffractive arrays are typically fabricated by e-beam lithography, but this is very time consuming and prone to defects. We investigated the feasibility of replicating such arrays using a custom step-and-flash imprint lithography (S-FIL) tool [1].

Imprint template patterns were fabricated as relief structures in bulk fused silica, using nickel liftoff after e-beam exposure of PMMA. The nickel pattern was used as a hardmask to dry etch the patterns into the underlying fused silica. After coating the template with a release layer, droplets of a low-viscosity imprint fluid were applied to the substrate surface, and the template was leveled and brought to within ~100 nm of the substrate. At that point the imprint fluid filled the template features via capillary action. The imprint fluid was crosslinked under UV exposure, and the template removed. The imprint process was completed in under 5 min. A two-step dry etch transferred the patterns into a transparent substrate. Figure 1 shows micrographs of the resulting imprinted and etched features [2].

The focusing capability of the imprinted diffractive elements was characterized by exposing single-spot features and comparing the feature width, or the derived point-spread function, with a finite-difference time-domain (FDTD) model, as illustrated in Fig. 2. We believe these experiments establish the efficacy of imprint lithography for reproduction of diffractive-optical arrays.

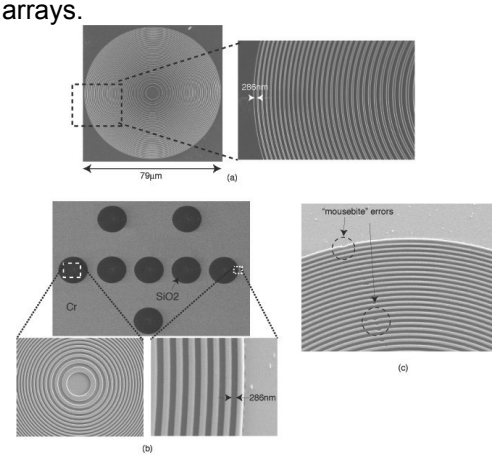

Figure 1: Scanning-electron micrographs of a zone plate imprinted in a fused silica substrate. (a) Imprinted pattern. (b) Etched pattern in fused silica. (c) Close-up view of etched patterns, indicating few local defects ("mousebites"). Moiré artefacts in the micrographs are generated by beating between the scan period of the SEM beam and the spatial periods of the zone plate.

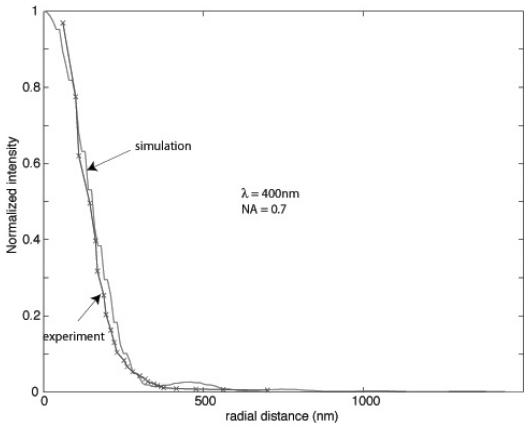

Figure 2: Point-spread function (PSF) characterization of the etched zone plates via single-spot exposures at increasing doses. After scaling, inverse diameters were plotted as a function of the dose. The FDTD-simulated PSF is also plotted for comparison. The parameters were λ = 400 nm, NA = 0.7, f = 40 μm. The data indicate the ability to achieve sub-wavelength focusing using imprinted zone plates.

References

[1] E.E. Moon, M.K. Mondol, P.N. Everett, and H.I. Smith, "Dynamic alignment control for fluid-immersion lithographies using interferometric-spatial-phase imaging," *J. Vac. Sci. Technol*. B **23**, p. 2607 (2005).

[2] M.D. Galus, E.E. Moon, H.I. Smith, and R. Menon, "Replication of diffractive-optical arrays via photocurable nanoimprint lithography," *J. Vac. Sci. Technol*. B **24**, p. 2960 (2006).

9. Interference Lithography

Sponsors
Internal funds

Project Staff
T.B. O'Reilly, H.I. Smith

Interference lithography (IL) uses the interference of 2 or more coherent light beams to produce periodic structures, such as gratings and grids. Typically, light from a laser is divided and recombined, forming a periodic intensity pattern that can be recorded in a photosensitive film (resist) on a substrate substrate. The NanoStructures Lab (NSL) has been developing interference lithography systems since the mid 1970's, and operates a range of tools for fabrication gratings, grids, and other periodic structures with periods as fine as 100 nm. These structures have a wide range of applications in nanoscale science and engineering. The most flexible and widely used of our IL systems is the Lloyd's mirror (LM). It can be easily configured to write patterns with periods from 170 nm to several microns. The LM system has recently been used to develop a simple and effective means of testing the response of photoresist to variations in image contrast and exposure dose. Other projects have used patterns from the LM to cut carbon nanotubes, guide the assembly of nanoparticles for templated self-assembly, study the behavior of strained-silicon, or fabricate templates for imprint lithography. The NSL also operates a Mach-Zehnder interferometer. Although this system lacks the flexibility and ease of use of the Lloyd's mirror, it produces higher quality patterns. The Mach-Zehnder system has been used to study in-plane distortion of silicon nitride membranes and to create super-prisms and super-collimators based on 2D photonic crystals. The NSL also operates an achromatic interference lithography (AIL) system. The AIL uses phase gratings to split and recombine the light from a pulsed, 193 nm ArF excimer laser. It produces 100 nm-period patterns, as shown in Figure 1. This system can form high-contrast fringe patterns over a large area, despite the limited temporal coherence of the ArF laser. The AIL system has been used to create free-standing gratings used in atom-beam interference experiments and EUV spectroscopy.

In addition, the NSL collaborates with the Space Nanotechnology Laboratory, which also operates a Mach-Zehnder IL system and the Nanoruler, an IL system that can write high-quality gratings over areas larger than 300 mm in diameter.

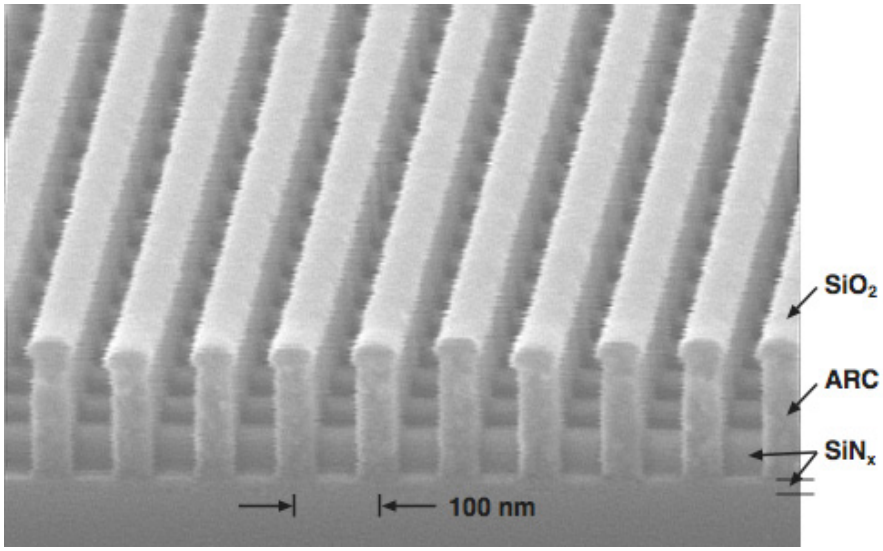

Figure 1: Scanning-electron micrograph of a stage in the fabrication of a 100 nm-period 2D grid, by means of two orthogonal exposures. Note that the underlying grating does not adversely affect the exposure control for the second, orthogonal grating on top.

10. Immersion-Achromatic-Interference Lithography

Sponsors
Singapore-MIT Alliance, SMA II

Project Staff
T.B. O'Reilly, M. Walsh, T. Savas, H.I. Smith

Interference lithography is a means of using the coherent interference of light to create periodic structures such as gratings and grids. The period of the pattern written is determined by the interference angle, θ, and the wavelength, λ, according to the equation $P = \lambda / 2n\sin(\theta)$. Since an upper limit exists for the interference angle (90°), to reduce the period below half the wavelength it is necessary to use an immersion fluid to reduce the effective wavelength of the light. The NanoStructures Lab is developing an immersion-interference-lithography system that will be capable of writing gratings with periods of 70 nm or even smaller.
The system under development, shown in Figure 1, is an achromatic grating interferometer similar to an existing system that is used to produce 100 nm-period gratings. Diffraction gratings are used split and recombine light in such a way that the contrast of the fringe pattern formed is not dependent on the source having high spatial or temporal coherence. Analysis of the proposed system has shown that it will be capable of writing gratings with periods as fine as 70 nm, over areas as large as the parent gratings, using water as the immersion fluid. Using immersion fluids of higher index, it should be possible to achieve grating periods as fine as 60 nm (i.e.. lines and spaces of 30 nm width). Gratings produced by this system will find application in areas such as atom interferometry, short-wavelength spectroscopy and templated self-assembly of macromolecules. In addition, the system will be used to study the performance of photoresists and immersion fluids at very high numerical apertures.

To produce a system with reasonable exposure times, the parent gratings must have high diffraction efficiency. Efficiency depends on the dimensions of the grooves that constitute the parent gratings. Diffraction from the gratings has been modeled using the rigorous-coupled-wave

analysis method. The resulting designs present a fabrication challenge, requiring the etching of high-aspect-ratio slots in silica glass. New processing techniques have been developed to produce such parent gratings.

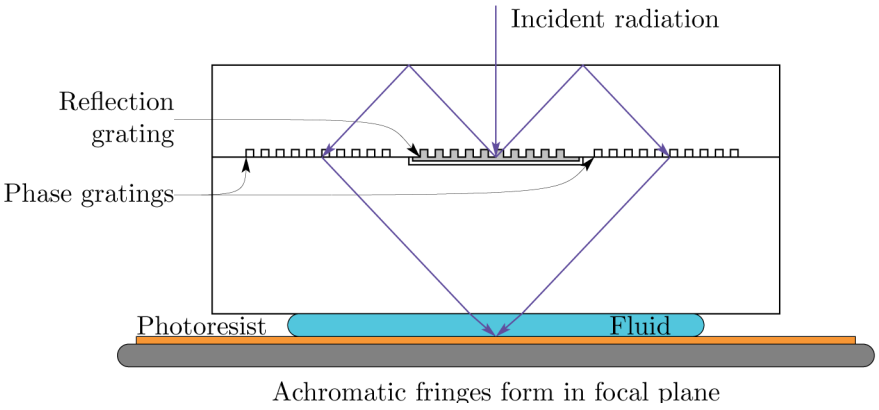

Figure 1: Immersion-achromatic-interference lithography system.

11. Sub-Nanometer Accuracy in Lateral Tip-to-Substrate Positioning for Scanning-Probe Lithography

Sponsors
Internal Funding

Project Staff
Dr. Euclid E. Moon, Prof. Karl Berggren, Prof. Henry I. Smith

In scanning-probe microscopy or lithography, a longstanding problem is that the lateral position of the tip relative to the substrate is subject to perturbations due to thermal expansion and other distortions in their long mechanical connection. Shortening the mechanical path to improve tip registration would limit a scanning probe to small substrates. Stiffening the mechanical connection has limited effectiveness. In either case, the tip-to-substrate position is unknown until scans are performed, and, as a result of the finite time required to complete a scan, mechanical distortions of tip-to-substrate position typically are evident between the completion of the scan and the subsequent positioning of the tip.

In this work we apply an interferometric position metrology technique, called Interferometric-Spatial-Phase Imaging (ISPI), to directly and continuously measure and control lateral tip-to-substrate position in a scanning-probe system, and demonstrate use of tip-to-substrate control for nanometer-precision lithography.

Simple modifications were made to adapt ISPI to a commercially available AFM (Veeco Dimension 3000), as shown in Fig. 1. Modifications include the addition of two ISPI microscopes, a super-invar tip holder with a fused-silica reference flat containing ISPI marks, and a closed-loop piezo stage with internal capacitive sensors under the substrate. Observing displacement with ISPI yields previously unattainable insight into the behavior of the tip relative to the substrate. Figure 2 illustrates tip-to-substrate behavior while attempting to hold the tip at a single point using (a) the open-loop piezo, (b) the closed-loop piezo, and (c) ISPI feedback to the substrate piezo stage to correct for unintended displacements. Figure 3 shows the ability to place the tip at a regular array of points, as well as repeatability, using each of the three tip positioning methods

(a), (b), (c). Figure 4 shows statistics for tip positioning at a grid array using ISPI. Lithography performed in a polymer with a tapping tip is shown in Fig. 5, in which two identical closed-path figures are described by the tip under ISPI control, directly on top of each other. Attempts at writing similar patterns without using ISPI position control result in overlay errors of several tens, or hundreds, of nanometers. We believe these experiments, among others, demonstrate the benefits of direct, continuous monitoring and control of tip-to-substrate position for nanolithography, as well as metrologically-accurate scanning-probe imaging.

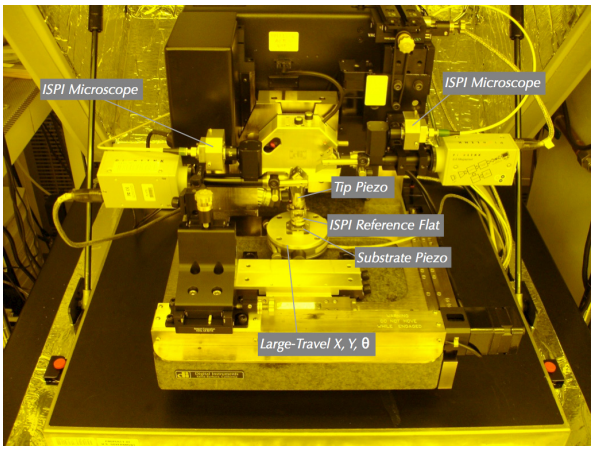

Figure 1: Photograph of the ISPI-modified AFM. The additional ISPI hardware consists of microscopes for measuring X and Y position, and a custom super-invar tip holder with ISPI marks. A closed-loop piezo stage replaces the substrate chuck.

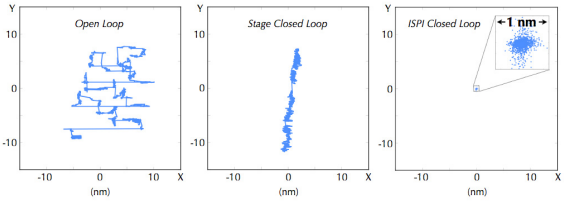

Figure 2: ISPI measurements of tip-to-substrate position while attempting to hold the tip at a single point over the substrate using (a) an open-loop piezo, (b) a closed-loop piezo stage, and (c) ISPI to feedback-control tip-to-substrate position. Although both open-loop and closed-loop piezo stages permit drift of more than 10 nm during 10 minutes, ISPI measurements indicate elimination of tip-to-substrate drift within $3\sigma = 0.3$ nm in X and $3\sigma = 0.4$ nm in Y.

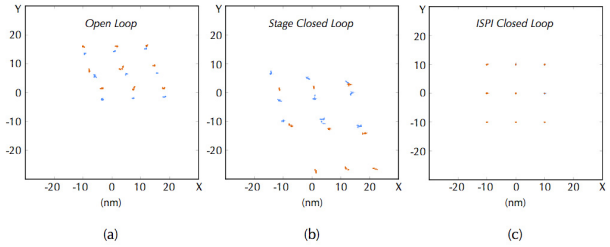

Figure 3: ISPI measurements of attempts to position a tip on a 3x3 grid, with 10 nm period. Data were taken using the (a) open-loop piezo; (b) closed-loop piezo; and (c) ISPI feedback control. In each case the tip was held at an intended position for 2 minutes, and then moved to the next point, following a serpentine scan, starting at the lower left point. The grid scan was repeated in the reverse order, as shown by a second set of points that are intended to overlay upon the first set. Errors amount to several nanometers, or tens of nanometers, with either open-loop or stage closed-loop operation. Data using ISPI control for the two grid scans are overlaid, and are indistinguishable, as shown in (c).

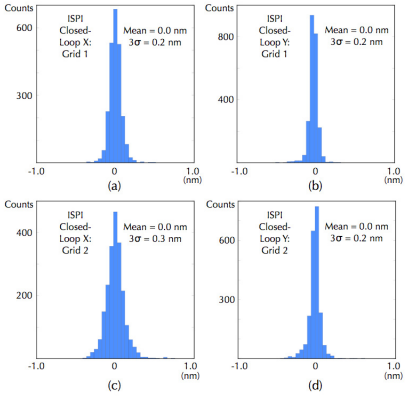

Figure 4: Plots of the disparity of ISPI positioning from the intended pattern placement, taken during position locking of the tip in the two successive grid scans shown in Fig. 3(c). (a), (b) ISPI control results in positioning at grid points with overlay disparities of 3σ = 0.2 nm in X and 3σ = 0.2 nm in Y. In the second grid scan (c), (d), the deviation from the desired positions was 3σ = 0.3 nm in X and 3σ = 0.2 nm in Y. The data show good placement accuracy within each grid scan, as well as good repeatability between successive scans. The mean position deviation was 0.0 nm in each scan.

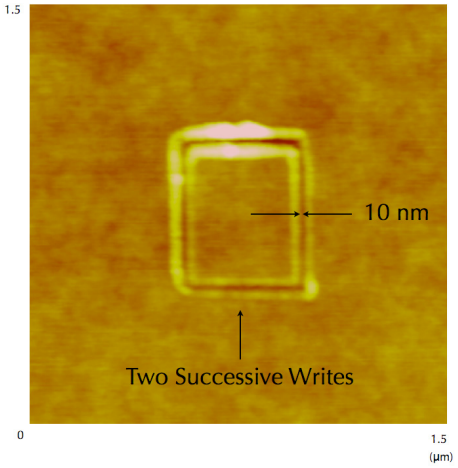

Figure 5: AFM scan of patterns written in PMMA showing overlay of two patterns using ISPI control. The double-patterned scan employing ISPI is indistinguishable from a single-patterned scan, indicating an upper bound on the overlay (<10 nm) that is limited by the lateral detectivity of the AFM (256x256 data points in a 1.5x1.5 μm scan).

References

[1] Euclid E. Moon and Henry I. Smith, "Nanometer-precision pattern registration for scanning-probe lithographies using interferometric-spatial-phase imaging," *J. Vac. Sci. Technol*. B **24**, 3083 (2006).

[2] Euclid E. Moon, Jan Kupec, Mark K. Mondol, Henry I. Smith, and Karl K. Berggren, "Atomic-force lithography with interferometric tip-to-substrate position metrology," Submitted for Publication, *J. Vac. Sci. Technol*. B **25** (2007).

12. Sub-10 nm Feature Resolution in Arbitrary Pattern Geometries Using Atomic-Force Lithography

Sponsors
Internal Funding

Project Staff
Dr. Euclid E. Moon, Prof. Henry I. Smith

Research in imprint lithography has demonstrated successful pattern transfer of 2 nm features from imprint templates to substrates. An open issue is imprint template fabrication at this resolution. Electron-beam lithography may be extendable to the sub-10 nm domain, however, limitations exist due to electron scattering and proximity effects. Helium-ion lithography can reach a theoretical resolution of ~1 nm, although this potential has yet to be demonstrated, and pattern registration at the sub-1 nm level remains an obstacle.

In this work we demonstrate a simple method of using a scanning probe tip to write sub-10 nm features [1] in a polymer, such as PMMA, on an imprint template.

We employ a tip with an additional self-assembled spike of carbon or tungsten. Tips are shown in Fig. 1 to be capable of resolving adjacent C_{60} molecules, indicating the tip diameter is <0.7 nm. Deconvolution of the tip shape with the known geometry of C_{60} molecules suggests a tip diameter of 0.28 nm, or approximately 3 carbon atoms.

During lithography, the tip is operated in tapping mode, albeit closer to the surface than in the conventional imaging mode. Figure 2 illustrates 10 nm half-pitch gratings written with the tip. Figures 3 and 4 show arbitrary patterns written with the tip, having FWHM linewidths of 9.3 nm and 2.9 nm, respectively. We will utilize sub-nanometer diameter tips with interferometric tip-to-substrate control, for sub-nanometer lateral positioning, as well as continuous interferometric tracking of tip height, a necessary factor for consistent linewidth control.

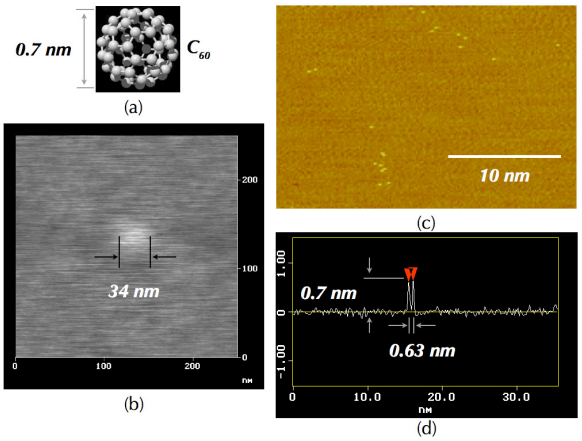

Figure 1: (a) Model of a C_{60} molecule. (b) AFM scan of a single fullerene (C_{60}) molecule using a conventional etched silicon tip. Convolution of the tip diameter with the molecule produces a 34 nm smear. (c) AFM scan of fullerene (C_{60}) molecules using a diamond-like carbon spike tip, demonstrating resolution of individual molecules. (d) Cross-section of a pair of fullerenes within Fig. 1(c), indicating the carbon tip diameter is less than the intermolecular distance (<0.7 nm).

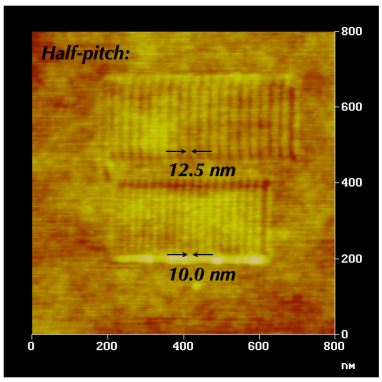

Figure 2: AFM scan of gratings written with a tungsten tip in PMMA. Grating half-pitch is 12.5 nm and 10.0 nm in the upper and lower gratings, respectively.

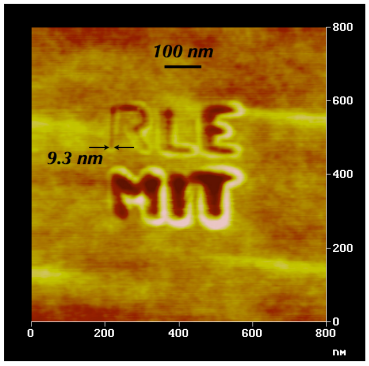

Figure 3: AFM scan of an arbitrary pattern written with a tungsten tip in PMMA on a fused silica imprint template. Measured FWHM linewidth is 9.3 nm. The residual substrate tilt and surface topography varied the linewidth during the lithography.

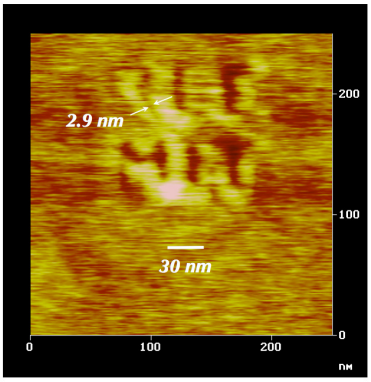

Figure 4: AFM scan of an arbitrary pattern written with a carbon tip in PMMA. Measured FWHM linewidth is 2.9 nm.

References

[1] Euclid E. Moon and Henry I. Smith, "Nanometer-precision pattern registration for scanning-probe lithographies using interferometric-spatial-phase imaging," *J. Vac. Sci. Technol*. B **24**, 3083 (2006).

13. Nanostructured Optical Fiber-to-Chip Couplers

Sponsors
DARPA

Project Staff
R. Barreto, M. Defosseux, C.W. Holzwarth, M. Araghchini, T. Barwicz, A.M. Khilo, M. Fan, M.A. Popovic, P.T. Rakich, M. Dahlem, E.P. Ippen, F.X. Kaertner, H. I. Smith

Efficient fiber-to-chip coupling is a significant problem for high-index-contrast (HIC) microphotonics due to the large difference in size and refractive index between the core of an optical fiber (several micrometers in diameter) and the core of a HIC waveguide (less than one micrometer wide). An efficient fiber-to-chip coupler is thus needed to match the mode of the fiber and transform it to a propagating mode within the HIC waveguide. We investigated two different approaches to accomplish the efficient coupling. In the first design, called a horizontal coupler, a large low-index polymer waveguide, with a mode diameter that nearly matches the mode diameter of an optical fiber, sits on a small high-index waveguide whose width tapers from <100 nm to the final desired width. This taper allows the optical power to be transferred adiabatically from the polymer waveguide to the high-index waveguide. Figure 1 shows a three-dimensional view of horizontal coupler designs for both an air clad silicon waveguide (a) and an overcladded silicon-rich silicon nitride (SiN_x) waveguide (b). For the overclad design the cladding must be selectively thinned from 1.6 □m to 0.1 □m in order to allow for efficient coupling between the polymer and SiN_x waveguides. We use Cyclotene as the material for the low-index polymer waveguide as shown in Figure 2. The second design, the vertical coupler, is based on a grating array composed of nanoscale elements that allow coupling from a vertically oriented fiber to a horizontally oriented waveguide. We are currently demonstrating this concept using SiN_x waveguides. Figure 3 shows a sketch of the vertical-coupler design requiring a two layer aligned process with a minimum feature size of ~100nm.

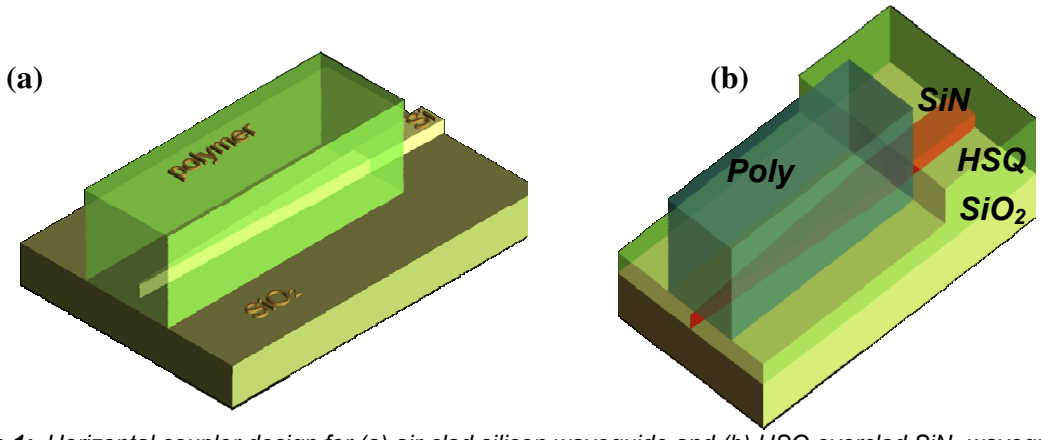

Figure 1: *Horizontal coupler design for (a) air-clad silicon waveguide and (b) HSQ overclad SiN_x waveguide using a selective overcladding thinning process.*

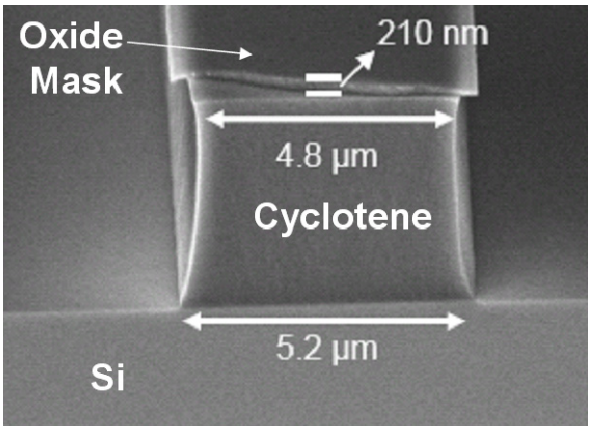

Figure 2: *Scanning-electron micrograph of Cyclotene waveguide used for the horizontal couplers.*

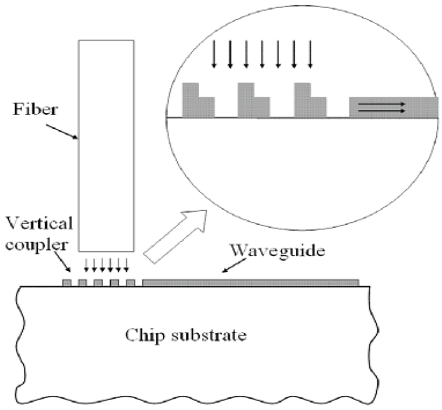

Figure 3*: Sketch of vertical coupler design.*

14. Nanofabrication of Optical Microring Filter Banks for Ultra-fast Analog-to-Digital Converters

Sponsors
DARPA

Project staff
C.W. Holzwarth, T. Barwicz, M.A. Popović, A.M. Khilo, P.T. Rakich, E.P. Ippen, F.X. Kärtner, and H.I. Smith

Microphotonic filter banks are an essential part of many proposed integrated photonic systems including ultra-fast analog-to-digital converters. Recent progress in designs and nanofabrication techniques for microring-resonators in high-index-contrast (HIC) materials have made possible the wide spectral spacing between resonances and low loss required for real world applications. Achieving accurate resonant-frequency spacing of microring-filters is critical for these devices. In the NanoStructures Laboratory we have developed fabrication techniques based on scanning-electron-beam lithography (SEBL), that enables accurate control of the resonant-frequency spacing of HIC microring-resonator filter banks.

Resonant frequency control in microring-resonator filters is achieved by controlling the optical path length of a ring, which depends on the ring's radius and the phase velocity of light in the ring. (The resonant frequency condition corresponds to there being an integral number of wavelengths around the ring.) The phase velocity depends on the width of the ring waveguide. To control the resonant frequency to within 1GHz, one must control the average width of the ring waveguide to within 10-50 pm, which is about 100 times finer than the minimum step size of the address grid of an SEBL system. To achieve this kind of width control, we adjusted the electron-beam dose.

In our experiments second-order microring-resonator filters fabricated in silicon-rich silicon nitride (SiN_x) were used in the microring filter banks (Figure 1). Calibration experiments were performed to find the filter's resonant frequency dependency on lithographic parameters such as the specified radius, width and exposure dose. Using dose modulation, eight-channel filter banks with channel spacing ranging from 90 to 180 GHz were fabricated and tested (Figure 2). The results demonstrate that we can accurately control a 2.7 nm change in average width of the ring waveguide to 0.11 nm, despite a 6 nm step size in the SEBL system [1].

As seen in Figure 2 the channel spacing is not exactly the same between every channel. This arises due to process variations that include slight variations of the SiN_x thickness, electron beam current fluctuations, and other random process variations. One way to correct this is to use thermal trimming, based on the thermo-optic coefficient of the refractive index, to correct for these errors. Our current efforts are focus on implementing thermal trimming into our filter bank design by placing heaters above the rings. Since the metallic heaters would cause the microring to have high loss we must overclad the microrings with a low-index material to optically isolate them from the heaters. We have developed a novel annealing process for HSQ to optimize its material properties for use as this overcladding material (Figure 3).

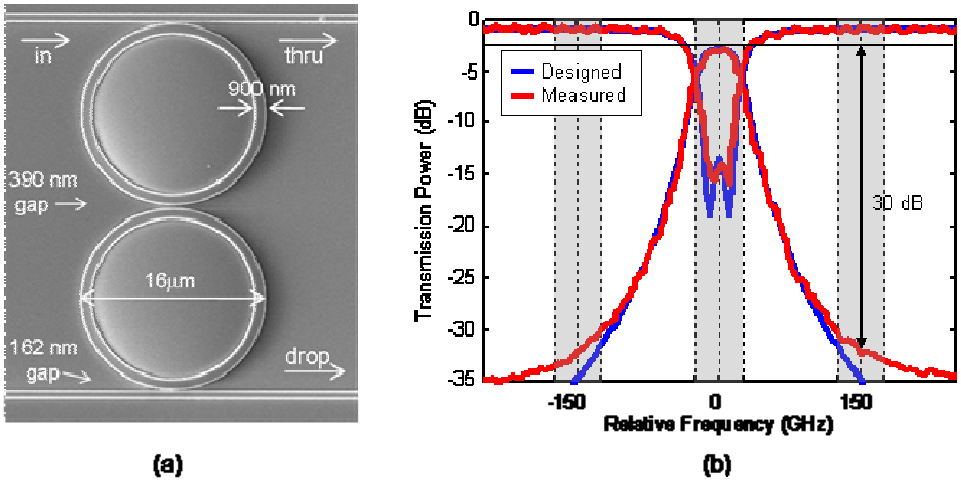

Figure 1: a) Scanning electron micrograph of a fabricated second-order microring-resonator filter with critical design dimension labeled. b) Designed and measured second-order microring resonator filter response that has a 20 nm free spectral range, 50 GHz bandwidth, 1.5 dB drop loss and less than 30 dB channel crosstalk.

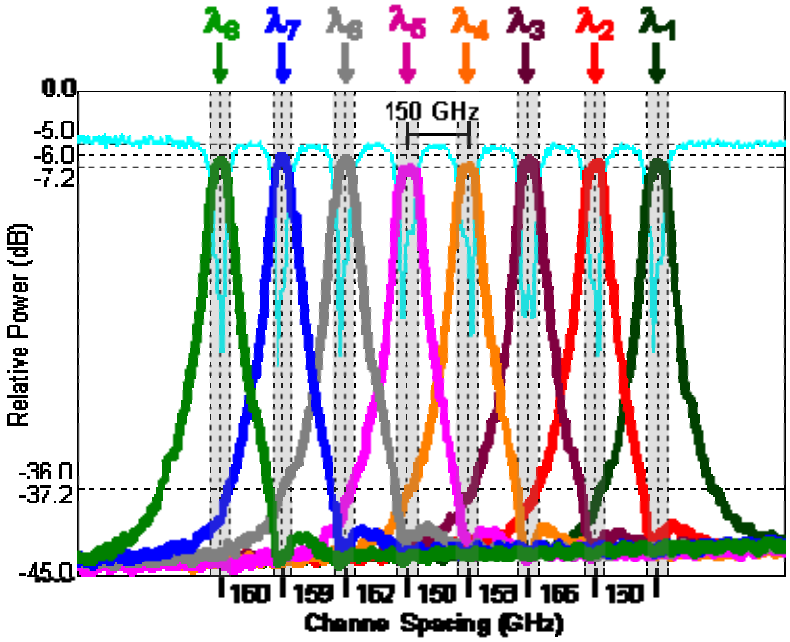

***Figure 2**: Measured response of an eight-channel filter bank based on second-order microring-resonators with a target channel spacing for 150 GHz. The actual average channel spacing measured is 159 GHz (σ = 5 GHz) and channel crosstalk is less than 30 dB.*

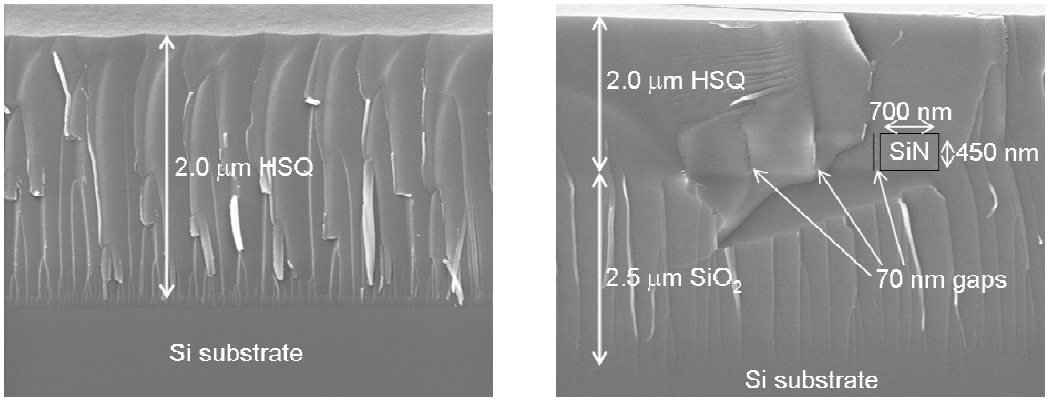

Figure 3: *(a) Scanning-electron micrograph of 2 □m thick overcladding layer made with HSQ using an optimized annealing process. (b) Scanning-electron micrograph demonstrating the gap-filling a planarization propertied of this optimized HSQ annealing process.*

References

[1] C.W. Holzwarth, T. Barwicz, M.A. Popovic, P.T. Rakich, E.P. Ippen, F.X. Kaertner and Henry I. Smith, "*Accurate resonant frequency spacing of microring filters without postfabrication trimming*," *JVST B Vol.* **24**, pp. 3244-3247 (2006).

15. Polarization-Transparent Optical Add-drop Multiplexers in Silicon Nitride

Sponsors

Pirelli S.p.A (Milan, Italy) and internal funds

Project Staff

T. Barwicz, M.R. Watts, M.A. Popovic, P.T. Rakich, C.W. Holzwarth, E.P. Ippen, F.X. Kaertner, H.I. Smith

Microphotonics promises to revolutionize optics through miniaturization and dense integration of optical elements on planar surfaces. Of particular interest are microphotonic devices that employ high refractive-index contrast (HIC). These devices have dimensions on the order of the optical wavelength and functionality often not achievable with macro-scale devices. A long-standing criticism of HIC microphotonic devices, however, is their inherent sensitivity to polarization, i.e., they respond differently to light polarized along different axes. Since the polarization state changes randomly in optical fibers, HIC microphotonic devices are incompatible with the optical fibers necessary to connect them to the outside world.

In the NanoStructures Laboratory, we have developed techniques that enable the fabrication of microphotonic devices, such as microring-based filters, that have unprecedented dimensional accuracy, resulting in unprecedented optical performance. In addition, we have overcome the problem of sensitivity to polarization by means of an integrated polarization-diversity scheme that renders the optical response of HIC microphotonic devices and systems insensitive to polarization. An optical add-drop multiplexer was realized and the polarization-dependent loss reduced to an average of 1 dB [2]. Figure 1 presents the optical circuit diagram implemented and electron micrographs of the structure. The optical response of the final device for the two eigenstates and fifty random polarizations is shown in Figure 2. The waveguides are fabricated in silicon-rich silicon nitride, and the critical dimensions vary from 70 to 3000 nm. The average

waveguide widths of the 18 microrings forming the add-drop multiplexer are matched to 0.15 nm. The aspect ratio of the tallest and thinnest structures reaches 12 to 1.

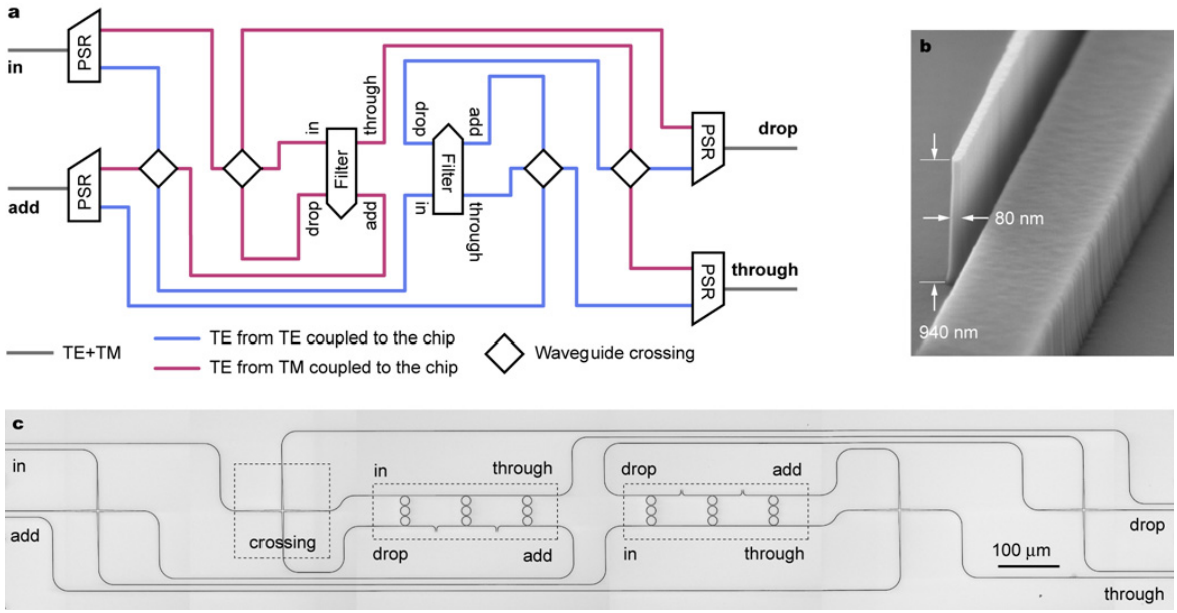

Figure 1: *(a) Optical circuit required to obtain a polarization insensitive optical response from polarization sensitive components. The acronym PSR stands for polarization splitter and rotator. The two filters shown in the schematic are identical. (b) Electron micrograph of the beginning end of the polarization splitter and rotator. (c) optical micrograph of the middle part of the circuit. The polarization splitters and rotators are not shown and extend to the right and the left of the micrograph. The grayscale was inverted to allow the fine lines to be readable when printed.*

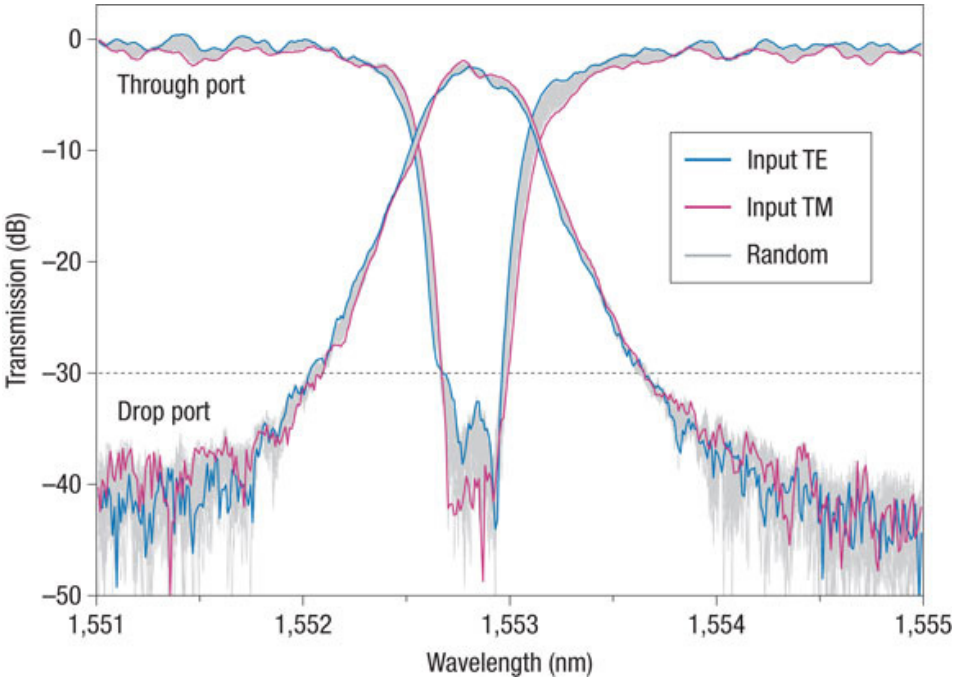

Figure 2: *Optical response of a polarization transparent optical add-drop filter demonstrating and average polarization dependant loss of 1dB. The two polarization eigenstates are shown in red and blue as well as 50 random polarizations shown in gray.*

References

[1] T. Barwicz, M.A. Popovic, M.R. Watts, P.T. Rakich, E.P. Ippen, and Henry I. Smith, "*Fabrication of add-drop filters based on frequency-matched microring-resonators*," *J. of Lightwave Technol. Vol.* **24**, pp. 2207-2218 (2006).

[2] T. Barwicz, M.A. Popovic, M.R. Watts, P.T. Rakich, L. Socci, E.P. Ippen, F.X. Kartner and Henry I. Smith, "*Polarization-transparent microphotonic devices in the strong confinement limit*," *Nature Photonics* Vol. **1**, pp. 57-60 (2007).

16. HITLESS RECONFIGURABLE OPTICAL ADD-DROP MULTIPLEXERS IN SILICON

Sponsors
Pirelli S.p.A (Milan, Italy) and internal funds

Project Staff
T. Barwicz, M.A. Popovic, F. Gan, M. Dahlem, C.W. Holzwarth, P.T. Rakich, E.P. Ippen, F.X. Kaertner, and H. I. Smith

Reconfigurable optical add-drop multiplexers (ROADMs) are key components of modern optical networks. Data in optical fibers is carried via numerous wavelengths, referred to as channels. ROADMs allow the rerouting (dropping) of a subset of the data channels traveling in an optical fiber and replacing these with new data streams (adding) that will be carried in the fiber at the previously rerouted wavelengths. "Reconfigurable" indicates that the subset of dropped channels can be changed in real time while the ROADM is in operation.

Previously, we developed nanofabrication techniques of unprecedented accuracy that allowed us to demonstrate, in silicon-rich silicon nitride, the most advanced microring filters reported to date [1]. In the present work, we employ silicon microrings to take advantage of the lower optical loss and high thermo-optical coefficient of silicon. The latter enables wide-range tuning of the wavelengths of operation of the ROADM by means of integrated heaters. Line-edge roughness is of critical concern in silicon waveguides as it translates into optical-propagation loss via scattering of the guided mode. We found that the smoothest waveguides are obtained using hydrogen silsesquioxane (HSQ) as an e-beam resist and etch-mask. Reactive ion etching was done in HBr. Figure 1 is an electron micrograph of the coupling region between a microring and a bus waveguide defined in HSQ. The patterning was done by dose-controlled scanning electron-beam lithography. Figure 2 presents a cross-sectional diagram and top-view micrograph of our implementation of a hitless silicon ROADM.

The basic structure in Figure 2b consists of a microring resonator with a two point coupling arm. By thermally tuning the coupling arm by a π phase shift it is possible to minimize the coupling coefficient. With the coupling coefficient minimized it is possible to tune the microring from one channel to another without affecting the amplitude and phase response of other channels, as is demonstrated in Figure 3.

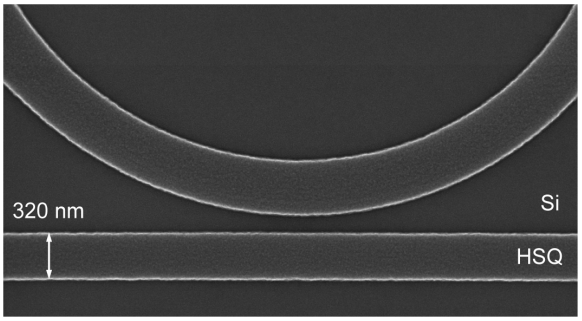

FIGURE 1: Top-view scanning-electron micrograph of a coupling region defined in HSQ. Line-edge smoothness is critical for Si waveguides. The patterning is based on scanning electron-beam lithography. The minimum feature size required is ~100 nm and must be controlled to ~ 5 nm.

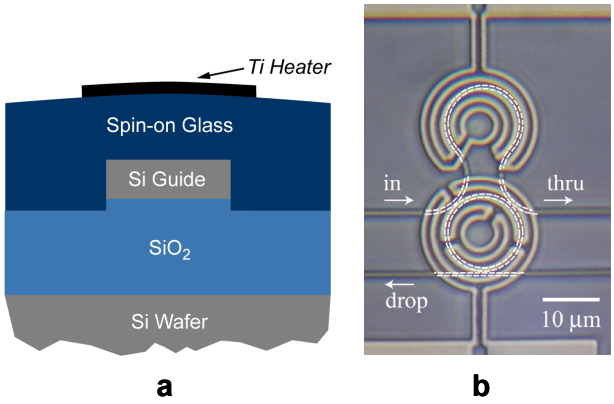

FIGURE 2: (a) Cross-sectional schematic of a silicon waveguide with an integrated titanium heater. Spin-on glass is used for the upper cladding of the waveguide to allow self-planarization and to avoid filling problems in narrow gaps. (b) Top-view optical micrograph of an overclad silicon-mcroring filter below a Ti heater.

References

[1] M.A. Popovic, T. Barwicz, M.R. Watts, P.T. Rakich, L. Socci, E.P. Ippen, F.X. Kaertner, and H.I. Smith, "*Multistage high-order microring-resonator add-drop filters*," to be published, *Optics Letters.*

17. Three-dimensional photonic crystals via membrane assembly

Sponsors
NSF

Project Staff
A. Patel and H. I. Smith

The diffraction of light within periodic structures (so called "photonic crystals") offers a wide variety of opportunities for controlling and manipulating light. Most research to date has focused on 2-dimensional (2D) photonic crystals, because highly developed planar-fabrication techniques (i.e., lithography followed by pattern transfer) are directly applicable. However, the full potential of photonic crystals in futuristic sensing, communication and computation systems is best achieved with 3-dimensional (3D) structures. The problem is that new methods of 3D fabrication need to be developed to achieve desired complex structures over large areas with low cost and high yield.

Interference lithography can produce periodic 3D structures in photosensitive polymers, but the introduction of deviations from perfect periodicity (i.e., waveguides and structures that constitute "devices" within the periodic matrix, so-called "defects") is highly problematic. Moreover, it's not clear that backfilling 3D polymeric structures is applicable to a suitable range of materials. Layer-by-layer methods enable the controlled introduction of defects, but to date fabrication is tedious, slow, low yield, and covers impractically small areas (e.g., <0.1mm on edge).

We describe a novel approach in which the 3D structure is fabricated by assembling membranes that are patterned in advance using conventional planar methods (Figure 1). This approach minimizes the yield problem because membranes can be inspected and selected before assembly, and the desired waveguides and devices, can be introduced at any level. When brought into contact, membranes that are free of particulate and other contamination will bond spontaneously by Van der Waals or other mechanisms.

We report progress to date using low-stress SiN_x membranes as the test vehicle. 2D periodic structures have been etched into-free standing membranes (Figure 2), and nonaligned stacking carried out (Figure 3). We do not consider precise alignment of layers a potential problem since light diffracted from the structures during assembly will provide a built-in, reliable alignment signal. We believe the major problem facing the membrane assembly approach will be ensuring freedom from particles and other contamination. Si membranes, with their higher refractive index, are more desirable and will be used in the next stage of our research.

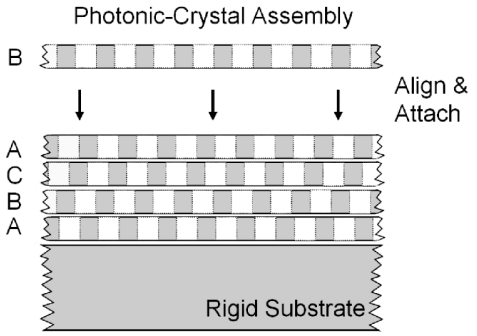

Figure 1: Depiction of the layer-by-layer stacking paradigm we are developing. All the layers in the photonic crystal are fabricated in parallel reducing processing cycles, which will help improve yield and reduce lead times.

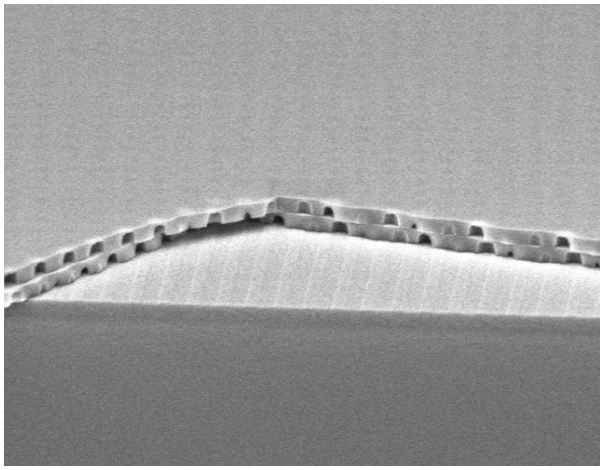

Figure 2: Initial stacking experiment. A patterned SiN membrane is brought into contact with SiN substrate. The pitch of the array is 600nm and the membrane is 350nm thick. A second patterned membrane is brought into contact.

18. Building Three-dimensional Nanostructures via Membrane Folding with Sub-Micron Alignment

Sponsors
Institute for Soldier Nanotechnologies, NSF Graduate Research Fellowships

Project Staff
W.J. Arora, A.J. Nichol, Prof. George Barbastathis, Prof. Henry I. Smith

We are investigating membrane-based methods of three-dimensional (3D) device fabrication. The general idea is to functionalize membranes with standard planar-fabrication processes and then fold or stack the membranes into a 3D structure. Our research is typically done on silicon nitride membranes (100-1000 nm-thick) for fabrication ease, but silicon membranes are also viable.

Ion implantation can be used to controllably fold membranes, because implanted ion concentrations exceeding about 10^{22} ions/cm^3 cause large compressive strains in the membrane,

on the order of 5%. These strains force the membrane to fold [1]. By varying the implanted ion energy, the implantation depth can be controlled and the stress can be concentrated in either the top or bottom of the membrane. This enables one to fold membranes either up or down as shown in Figure 1. We used helium ions in our experiments because they cause negligible sputter damage and can be implanted to depths of 20 to 200nm with low voltages (2-20 kV). Figure 2 shows additional folded structures obtained from experiment.

Magnetic forces can be used to both fold and align nanopatterned membranes [2]. Silicon nitride membranes of 1μm thickness and 100μm×100μm area were patterned with arrays of 75nm thick cobalt nanomagnets. The membrane segments were then patterned and released from the substrate, making them free to rotate about compliant torsional hinges. A schematic of the folding process is shown in Figure 3(a-c). Before folding, a 0.2 tesla external field magnetized the nanomagnets (a) along their long axis. The field was then rotated 180^{o} to create a magnetic torque to fold the membranes (b). This resulted in the membranes completely folding over into a coarse layer-to-layer alignment of 2μm.

After coarse alignment is achieved via folding, the nanomagnet arrays on the folded segments interact resulting in a very precise self-aligning force between arrays (c). Figure 3d shows the alignment results for folding ten samples. As shown in the plot, the magnet array interaction resulted in alignment error of roughly 200nm. Therefore, the coarse alignment was reduced by a factor of ten. Figure 4(a-b) show a scanning electron micrograph of aligned membranes. As shown in Figure 4c, the membranes can be made to align one full period off. Furthermore, the membrane alignment was reconfigurable because the external field could be used to unlatch, realign and latch the membranes. This was experimentally demonstrated over 50 times with a folded membrane sample. Finally, we have modeled the dynamics and found that the alignment accuracy can actually be much better than the lithographic patterning accuracy. Therefore, this method may be useful for 3D nano-systems that need feature placement accuracy better than 20nm such as 3D nanophotonics, 3D integrated circuits, and 3D memory.

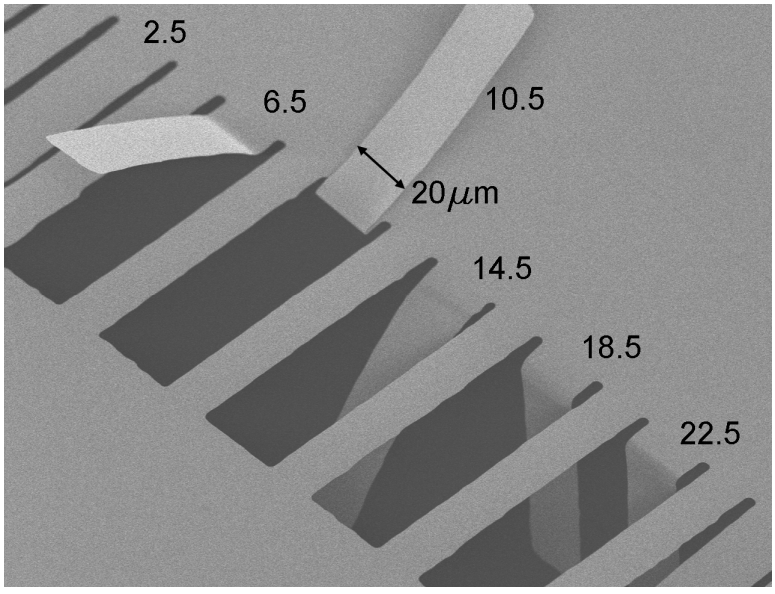

Figure 1: A 150nm-thick silicon nitride membrane was patterned into 20x100μm cantilevers and implanted with He^{+} ions. Implanted areas were 4x20μm and received an ion dose of $2.5x10^{17}$ ions/cm^{2}. This picture was taken from the backside of the membrane for clarity. The implantations were conducted from the topside of the membrane. The number next to each cantilever is the He^{+} ion energy in keV. Higher energy implants folded the membranes up and lower energy implants folded the membranes down.

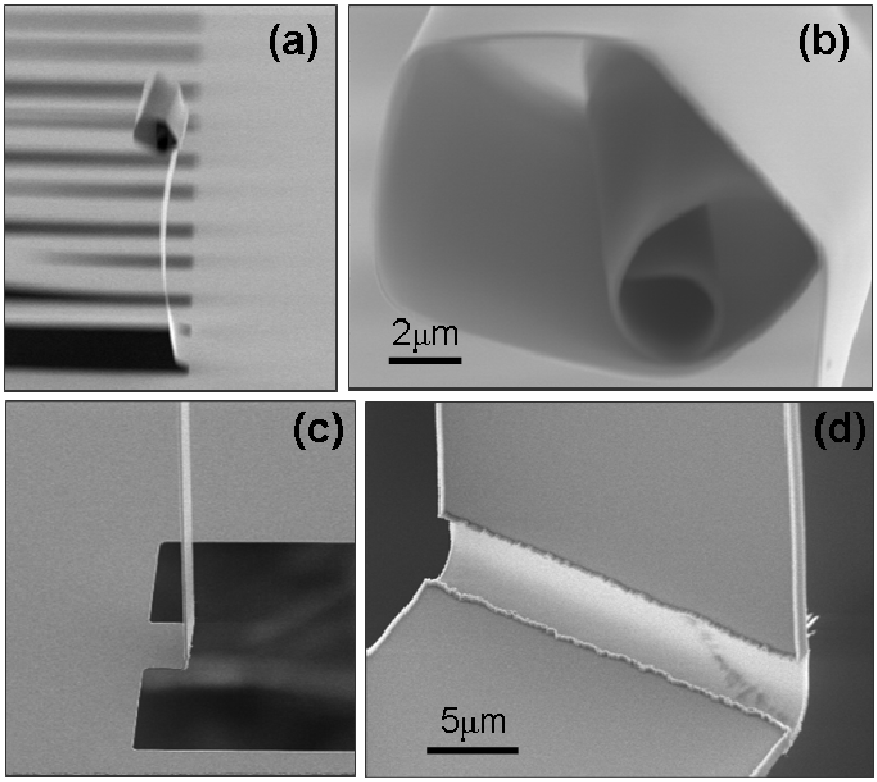

Figure 2: *(a, b) Starting from the free end, multiple downward folds curled the membrane into the spiral structure. The upward fold at the base shows that bi-directional folding is possible on the same cantilever. (c, d) Thicker membranes are straighter and more useful for building devices. This 600nm-thick membrane was thinned to 100nm to only allow folding at that location.*

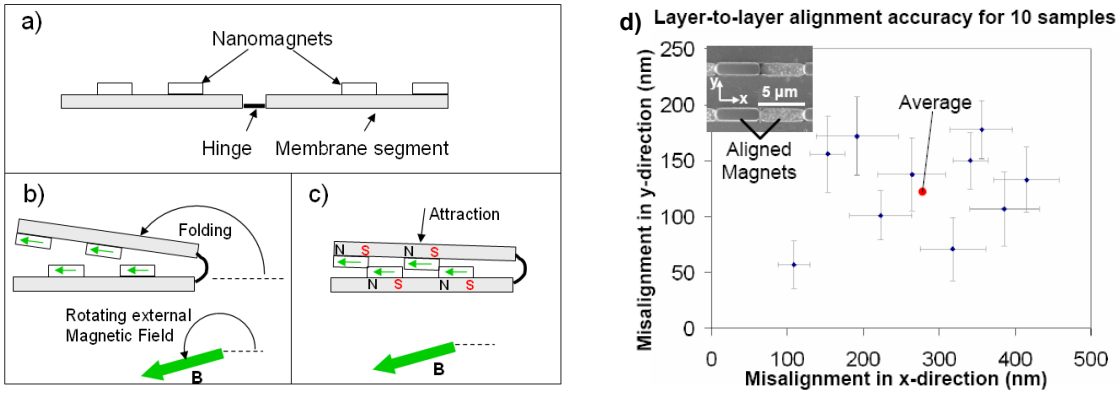

Figure 3: *(a-c) Schematic of the nanomagnet folding and alignment method. Nanomagnets placed on membranes are first magnetized (a) and then folded (b) with a rotating magnetic field. When the membranes are within a coarse alignment, the nanomagnets attract and self-align (c). The layer-to-layer alignment error for 100μm ×100μm ×1 μm SiN_x membranes that were folded and aligned using arrays of nanomagnets and an external magnetic field is shown in (d).*

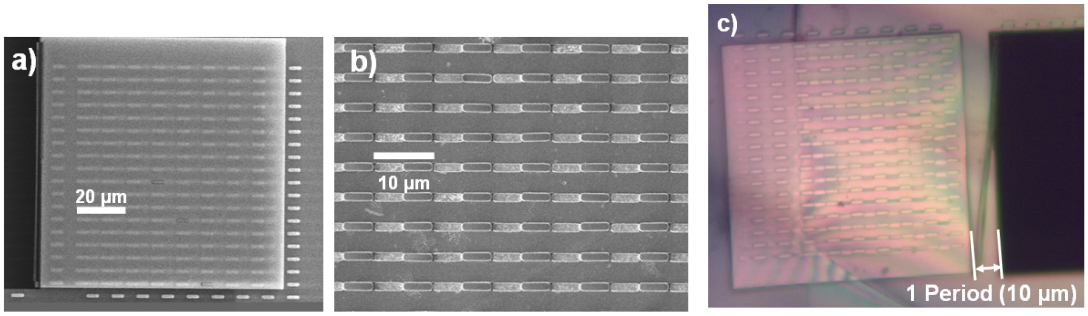

Figure 4: (a) Scanning electron micrograph of a membrane folded over and aligned to a nanomagnet array on the substrate. (b) The top membrane has been etched away leaving the nanomagnets. (c) Example of the membranes self-aligning one period off due to a large initial coarse alignment.

References

[1] W.J. Arora, H.I. Smith, and G. Barbastathis. "Membrane folding by He^+ ion implantation for three-dimensional device fabrication," Submitted for publication to *J. Vac. Sci. & Tech. B,* 2007.

[2] A.J. Nichol, P.S. Stellman, W.J. Arora, G. Barbastathis, "Two-step magnetic self-alignment of folded membranes for 3D nanomanufacturing," Microelec. Eng., 84, 5-8, 1168 (2007).

19. Nanometrology

Sponsors

NSF

Project Staff

R. Heilmann, J. Montoya, Y. Zhao, D. Trumper and M.L. Schattenburg

Manufacturing of future nanodevices and systems will require accurate means to pattern, assemble, image and measure nanostructures. Unfortunately, the current state-of-the-art of dimensional metrology, based on the laser interferometer, is grossly inadequate for these tasks. While it is true that when used in carefully-controlled conditions interferometers can be very precise, they typically have an accuracy measured in microns rather than nanometers. Achieving high accuracy requires extraordinarily tight control of the environment and thus high cost. Manufacturing at the nanoscale will require new technology for dimensional metrology which enables sub-1 nm precision and accuracy in realistic factory environments.

A recently formed MIT-UNC–Charlotte team is developing new metrology technology based on large-area grating patterns that have long-range spatial-phase coherence and ultra-high accuracy. Our goal is to reduce errors in gratings by 10-100 times over the best available today. These improved gratings can be used to replace interferometers with positional encoders to measure stage motion in a new nanomanufacturing tools, and to calibrate the dimensional scales of existing nanofabrication tools. This increased precision and accuracy will enable the manufacturing of nanodevices and systems that are impossible to produce today. Improved dimensional accuracy at the nano-to-picometer scale will have a large impact in many nanotechnology disciplines including semiconductor manufacturing, integrated optics, precision machine tools and space research.

As part of this effort, we will utilize a unique and powerful tool recently developed at MIT called the Nanoruler that can rapidly pattern large gratings with a precision well beyond other methods.

Another unique high-precision tool, the UNCC-MIT-built Sub-Atomic Measuring Machine (SAMM), is being brought to bear to research new ways to quantify and reduce errors in the gratings.

Recent work at MIT is focused on improving the thermal controls in the Nanoruler lithography enclosure and developing an improved interferometer system to reduce errors in the stage metrology frame. At UNCC the SAMM is undergoing extensive refurbishment and improvements designed to boost interferometer accuracy.

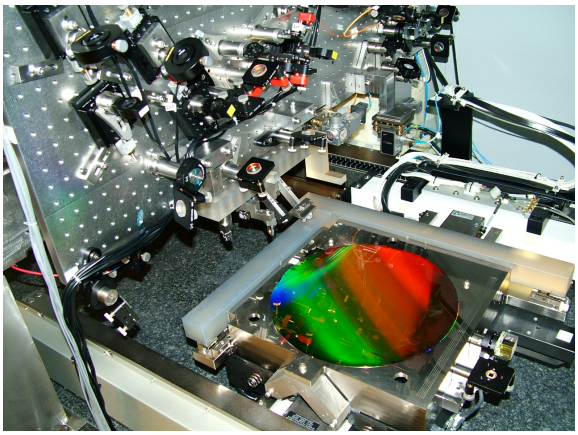

Figure 1: Photograph of the Nanoruler lithography and metrology system built by MIT students. This unique tool is the most precise grating patterning and metrology system in the world.

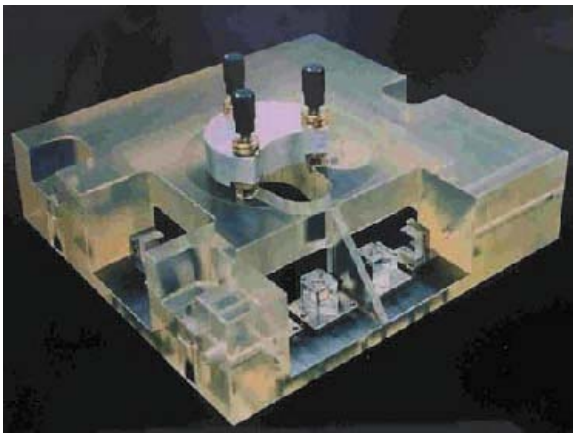

Figure 2: Photograph of reference block/sample holder for the Sub-Atomic Measuring Machine at the University of North Carolina – Charlotte.

References

[1] "Nanometer-level repeatable metrology using the Nanoruler," P. Konkola, C. Chen, R.K. Heilmann, C. Joo, J. Montoya, C.-H. Chang and M.L. Schattenburg, *J. Vac. Sci. Technol. B* **21**, 3097-3101 (2003).

[2] "Dimensional metrology for nanometer-scale science and engineering: towards sub-nanometer accurate encoders," R.K. Heilmann, C.G. Chen, P.T. Konkola and M.L. Schattenburg, *Nanotechnology* **15**, S504-S511 (2004).

[3] "Measuring two-axis stage mirror non-flatness using linear/angular interferometers," J. Montoya, R.K. Heilmann and M.L. Schattenburg, *Proc. of the 19th Annual Meeting of the American Society for Precision Engineering*, Vol. **34**, 382-385 (2004).

[4] "Measurement of milli-degree temperature gradients in environmental enclosures," Y. Zhao, C.-H. Chang, J. Montoya, R.K. Heilmann and M.L. Schattenburg, *Proc. of the 20th Annual Meeting of the American Society for Precision Engineering*, Vol. **37**, 226-229 (2005).

20. Scanning Beam Interference Lithography

Sponsors

NASA, Plymouth Grating Laboratory

Project Staff

M. Ahn, C.-H. Chang, R. Heilmann, Y. Zhao and M.L. Schattenburg

Traditional methods of fabricating gratings, such as diamond tip ruling, electron and laser beam scanning, or holography, are generally very slow and expensive and result in gratings with poor control of phase and period. More complex periodic patterns, such as gratings with chirped or curved, lines, or 2D and 3D photonic patterns, are even more difficult to pattern. This research program seeks to develop advanced interference lithography tools and techniques to enable the rapid patterning of general periodic patterns with much lower cost and higher fidelity than current technology.

Interference lithography (IL) is a maskless lithography technique based on the interference of coherent beams. Interfering beams from an ultra-violet laser generates interference fringes which are captured in a photo-sensitive polymer resist. Much of the technology used in modern IL practice is borrowed from technology used to fabricate computer chips. Traditional IL methods result in gratings with large phase and period errors. We are developing new technology based on interference of phase-locked scanning beams, called scanning beam interference lithography (SBIL). The SBIL technique has been realized in a tool called the MIT Nanoruler, which recently won a R&D 100 award (Fig. 1). Large gratings can be patterned in a matter of minutes with a grating phase precision of only a few nanometers and a period error in the ppb range (Fig. 2).

Current research efforts seek to generalize the SBIL concept to pattern more complex periodic patterns, such as variable period (chirped) gratings, 2D metrology grids, and photonic patterns [1]. Important applications of large, high fidelity gratings are for high-resolution x-ray spectroscopes on NASA x-ray astronomy missions, high energy laser pulse compression optics, and length metrology standards. We are in the process of a major upgrade of the Nanoruler optical and mechanical system which will allow rapid variation and control of grating pitch and fringe orientation, which will enable a new mode of operation of the Nanoruler that we call variable-period SBIL.

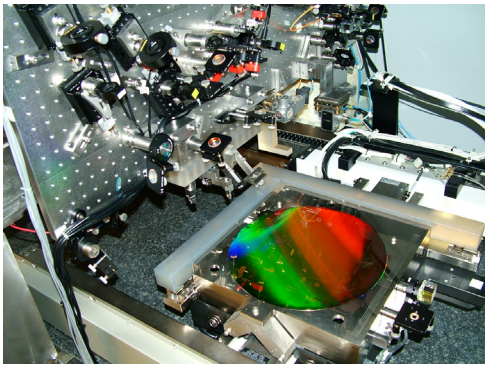

Figure 1: Photograph of the Nanoruler lithography and metrology system built by MIT students. This unique tool is the most precise grating patterning and metrology system in the world.

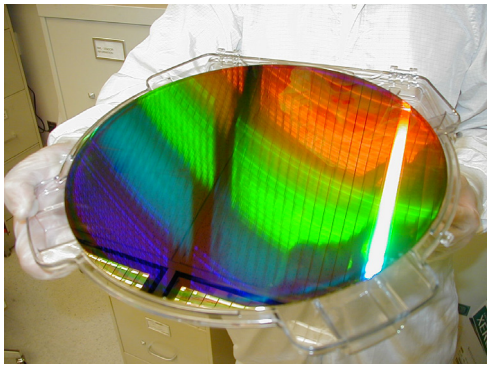

Figure 2: A 300 mm-diameter silicon wafer patterned with a 400 nm-period grating by the Nanoruler. The grating is diffracting light from the overhead fluorescent bulbs.

References

[1] "A generalized scanning beam interference lithography system for patterning gratings with variable period progressions," G.S. Pati, R.K. Heilmann, P.T. Konkola, C. Joo, C.G. Chen, E. Murphy and M.L. Schattenburg, J. Vac. Sci. Technol. B 20, 2617-2621 (2002).

[2] "Nanometer-level repeatable metrology using the Nanoruler," P. Konkola, C. Chen, R.K. Heilmann, C. Joo, J. Montoya, C.-H. Chang and M.L. Schattenburg, *J. Vac. Sci. Technol. B* **21**, 3097-3101 (2003).

[3] "Doppler writing and linewidth control for scanning beam interference lithography," J. Montoya, C.-H. Chang, R.K. Heilmann and M.L. Schattenburg, *J. Vac. Sci. Technol. B* **23**, 2640-2645 (2005).
[4] "Advanced heterodyne fringe-locking system using multiple frequency shifts," C.-H. Chang, R.K Heilmann and M.L. Schattenburg, *Proc. of the 20th Annual Meeting of the American Society for Precision Engineering*, Vol. **37**, 375-378 (2005).

21. Nanofabricated Reflection and Transmission Gratings

Sponsors:
NASA

Project Staff:
M. Ahn, C.-H Chang, R. Heilmann, J. Montoya, Y. Zhao, Prof. M.L. Schattenburg

Diffraction gratings and other periodic patterns have long been important tools in research and manufacturing. Diffraction is due to the coherent superposition of waves—a phenomena with many useful properties and applications. Waves of many types can be diffracted, including visible and ultraviolet light, x-rays, electrons and even atom beams. Periodic patterns have many useful applications in fields such as optics and spectroscopy, filtering of beams and media, metrology, high-power lasers, optical communications, semiconductor manufacturing, and nanotechnology research in nanophotonics, nanomagnetics and nanobiology.

The performance of a grating is critically dependant on the geometry of individual grating lines. Lines can have rectangular, triangular or other geometries, depending on the application. High efficiency requires control of the geometric parameters which define individual lines (e.g., width, height, smoothness, sidewall angle, etc.) in the nanometer or even sub-nanometer range. For some applications control of grating period in the picometer to femtometer range is critical. Traditional methods of fabricating gratings, such as diamond tip ruling, electron and laser beam scanning, or holography, generally result in gratings which fall far below theoretical performance limits due to imperfections in the grating line geometry. The main goal of our research is to develop new technology for the rapid generation of general periodic patterns with control of geometry measured in the nanometer to sub-nanometer range in order to achieve near-theoretical performance and high yields.

Fabrication of gratings is generally accomplished in two main steps, (1) lithographic patterning into a photosensitive polymer resist, followed by (2) pattern transfer. A companion research program in this report entitled *Scanning Beam Interference Lithography* describes progress in advanced grating patterning. In this abstract we report on research in pattern transfer technology. Development of a variety of grating geometries and materials is ongoing. Advanced gratings have been fabricated for 10 NASA missions, and further advances are sought for future missions [1]. Fig. 1 depicts a gold wire-grid transmission grating designed for filtering deep-UV radiation for atom telescopes, while Fig. 2 depicts a nano-imprinted saw-tooth reflection grating for x-ray spectroscopy.

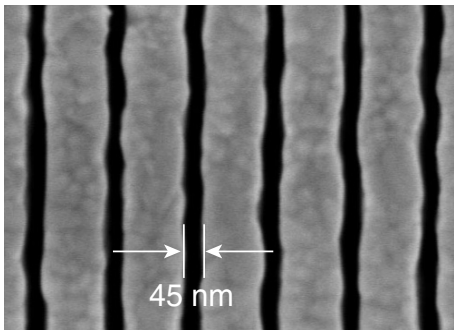

Figure 1: Scanning-electron micrograph of a deep-UV blocking grating used in atom telescopes on the NASA IMAGE and TWINS missions. The grating blocks deep-UV radiation while passing energetic neutral atoms.

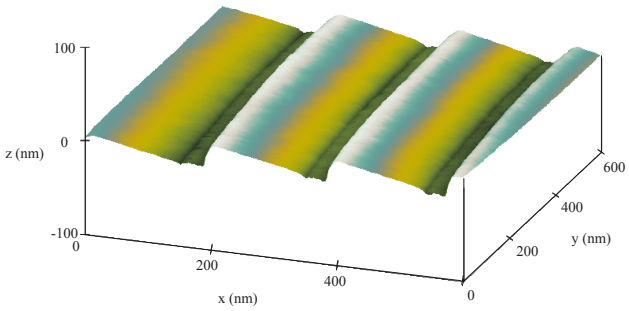

Figure 2: AFM image of 200 nm-period nano-imprint grating with 7° blaze angle developed for the NASA Constellation X mission. The groove surfaces are extremely smooth with a RMS surface roughness of <0.2 nm.

References

[1] "From nanometers to gigaparsecs: the role of nanostructures in unraveling the mysteries of the cosmos," M.L. Schattenburg, *J. Vacuum Sci. Technol. B* **19**, 2319-2328 (2001).

[2] "Fabrication of saw-tooth diffraction gratings using nanoimprint lithography," C.-H. Chang, R.K. Heilmann, R.C. Fleming, J. Carter, E. Murphy, M.L. Schattenburg, T.C. Bailey, R.D. Frankel and R. Voisin, *J. Vac. Sci. Technol. B* **21**, 2755-2759 (2003).

[3] "High fidelity blazed grating replication using nanoimprint lithography," C.-H. Chang, J.C. Montoya, M. Akilian, A. Lapsa, R.K. Heilmann, M.L. Schattenburg, M. Li, K.A. Flanagan, A.P. Rasmussen, J.F. Seely, J.M. Laming, B. Kjornrattanawanich and L.I. Goray, *J. Vac. Sci. Technol. B* **22**, 3260- 3264 (2004).

[4] "Near-normal-incidence extreme-ultraviolet efficiency of a flat crystalline anisotropically etched blazed grating," M.P. Kowalski, R.K. Heilmann, M.L. Schattenburg, C.-H. Chang, F.B. Berendse and W.R. Hunter, *Applied Optics* **45**, 1676-1679 (2006).

[5] "Efficiency of a grazing-incidence off-plane grating in the soft x-ray region," J. F. Seely, L. I. Goray, B. Kjornrattanawanich, J. M. Laming, G. E. Holland, K. A. Flanagan, R. K. Heilmann, C.-H. Chang, M. L. Schattenburg, and A. P. Rasmussen, *Applied Optics* **45**, 1680-1687 (2006).

Publications

Journal Articles, Published

1. T. Barwicz, M. A. Popovic, M.R. Watts, P.T. Rakich, E.P. Ippen and H.I. Smith, "Fabrication of add-drop filters based on frequency-matched microring-resonators," Journal of Lightwave Technology, Vol. 24, No. 5, 2207-2218 (2006).
2. R. Menon, D. Gil, H. I. Smith "Experimental Characterization of Focusing by High-Numerical-Aperture Zone Plates", J. Opt. Soc. Amer., Vol. 23, No. 3, pp. 567-571 (2006).
3. W.J. Arora, A.J. Nichol, H.I. Smith, and G. Barbastathis. "Membrane-folding to achieve three-dimensional nanostructures," Appl. Phys. Lett., **88**, p. 053108, (2006).
4. H. I. Smith, R. Menon, A. Patel, D. Chao, M. Walsh, G. Barbastathis, "Zone-plate-array lithography: a low-cost complement or competitor to scanning-electron-beam lithography," Microelectronic Engineering, vol.83, pp.956-961 (2006).

5. J.Y. Cheng, F. Zhang, H.I. Smith, G.J. Vancso, C.A. Ross, “Pattern registration between spherical block copolymer domains and topographical templates”, Advanced Materials **18**, 587-601 (2006).

6. C.A. Ross, F.J. Castaño, D. Morecroft, W. Jung, Henry I. Smith, T.A. Moore, T.J. Hayward, J.A.C. Bland, T.J. Bromwich, and A.K. Petford-Long,” Mesoscopic Thin Film Magnetic Rings (invited), “ J Appl. Phys. Vol. 99, 08S501 1-6 (2006).

7. C.W. Holzwarth, T. Barwicz, M.A. Popovic, P.T. Rakich, E.P. Ippen, F.X. Kaertner, H. I. Smith, “Accurate resonant frequency spacing of microring filters without postfabrication trimming,” J. Vac. Sci. Technol. B, 24(6), 3244-3247 (2006).

8. Matthias D. Galus, Euclid Moon, Henry I. Smith, Rajesh Menon, "Replication of diffractive-optical arrays via step-and-flash nano-imprint lithography,” J. Vac. Sci. Technol. 24(6), 2960-2963 (2006).

9. E.E. Moon, P.N. Everett, H.I. Smith, "Nanometer-precision pattern registration for scanning-probe lithographies using interferometric-spatial-phase imaging", J. Vac. Sci. Technol, Vol 24, (6), pp. 3083-3087 (2006).

10. Joy Y. Cheng, Caroline A. Ross, Henry I. Smith, Edwin L. Thomas, “Templated Self-Assembly of Block Copolymers: Top-Down Helps Bottom-Up,” Advanced Materials, 18, 2505-2521, (2006).

11. R. Menon and H. I. Smith, "Absorbance-modulation optical lithography," J. Opt. Soc. Amer. A **23**, pp. 2290-2294 (2006).

12. V.P. Chuang, J.Y. Cheng, T.A. Savas, C.A. Ross,” Three-dimensional Self-assembly of spherical block copolymer domains into V-shaped grooves.” Nano Letts. 6 (10), 2332 - 2337, (2006)

13. M. A. Popovíc, T. Barwicz, M. R. Watts, P. T. Rakich, L. Socci, E. P. Ippen, F. X. Kärtner, and H. I. Smith, "Multistage high-order microring-resonator add-drop filters," Opt. Lett. **31**, 2571-2573 (2006).

14. P. T. Rakich, M. A. Popovic, M. R. Watts, T. Barwicz, H. I. Smith, and E. P. Ippen, "Ultrawide tuning of photonic microcavities via evanescent field perturbation," Opt. Lett. **31**, 1241-1243 (2006).

15. Rajesh Menon, Hsin-Yu Tsai, Samuel W. Thomas III, “Far-Field Generation of Localized Light Fields using Absorbance Modulation,” Phys. Rev. Lett., 98, 043905 (2007).

16. Tymon Barwicz, Michael R. Watts, Miloš A. Popovic, Peter T. Rakich, Luciano Socci, Franz X. Kärtner, Erich P. Ippen, Henry I. Smith “Polarization-transparent microphotonic devices in the strong confinement limit,” Nature Photonics, Vol. 1, Issue 1, pp. 57-60 (2007).

17. T. Barwicz, H. Byun, F. Gan, C.W. Holzwarth, M.A. Popović, P.T. Rakich, M.R. Watts, E.P. Ippen, F.X. Kärtner, H.I. Smith, J.S. Orcutt, R.J. Ram, V. Stojanović, O.O. Olubuyide, J.L. Hoyt, S. Spector, M. Geis, M. Grein, T. Lyszczarz and J.U. Yoon, “Silicon photonics for compact, energy-efficient interconnects (inv),” J. Opt. Netw. 6, 63-73 (2007)

18. W. J. Arora, H. I. Smith, G. Barbastathis, “Membrane folding by ion implantation-induced stress to fabricate three-dimensional nanostructures ,” Microelectronic Engineering **84**, pp. 1454-1458 (2007).

Journal Articles, Submitted for Publication

1. F. Y. Ogrin, S.M. Weekes, B. Cubitt, A. Wildes, A. Drew, C.A. Ross, W. Jung, R. Menon," PNR investigation of periodic magnetic rings," J. Appl. Phys. In press (2007).

2. M.A. Popovic, M.R. Watts, T. Barwicz, P.T. Rakich, L. Socci, E.P. Ippen, F.X. Kartner and H.I. Smith, "High-index-contrast, wide-FSR microring-resonator filter design and realization with frequency-shift compensation", Optics Express, submitted for publication (2006).

3. I. Bita, T. Choi, M. E. Walsh, H. I. Smith and E. L. Thomas, "Large-area 3D Nanostructures with Octagonal Quasicrystalline Symmetry via Phase Mask Lithography," Advanced Materials in press.

4. H-Y. Tsai, H. I. Smith, R. Menon, "Fabrication of spiral-phase diffractive elements using scanning-electron beam-lithography," To be published, J. Vac. Sci. Technol. B, Nov/Dec (2007)

5. E. E. Moon, J. Kupec, M. K. Mondol, H. I. Smith and K. K. Berggren, "Atomic-force lithography with interferometric tip-to-substrate position metrology," to be published J. Vac. Sci. Techno. B, Nov/Dec 2007.

6. W. J. Arora, S. Sijbrandij, L. Stern, J. Notte, H. I. Smith and G. Barbastathis, "Membrane folding by He+ ion implantation for three-dimensional device fabrication," to be published J. Vac. Sci. Techno. B, Nov/Dec 2007.

7. A. A. Patel and H. I. Smith, "Membrane stacking: A new approach for three-dimensional nanostructure fabrication," to be published J. Vac. Sci. Techno. B, Nov/Dec 2007.

8. T. B. O'Reilly and H. I. Smith, "Characterization of photoresist using double-exposure with interference lithography," to be published J. Vac. Sci. Techno. B, Nov/Dec 2007.

9. C. Holzwarth, T. Barwicz and H. I. Smith, "Optimization of hydrogen silsesquioxane films for photonic applications," to be published J. Vac. Sci. Techno. B, Nov/Dec 2007.

Conference Presentations:

1. S.J. Spector, T.M. Lyszczarz, M.W. Geis, D.M. Lennon, J.U. Yoon, M.E. Grein, R.T. Schulein, F.X. Kärtner, R. Amatya, G. Barbastathis, H. Byun, F. Gan, C.W. Holzwarth, J.L. Hoyt, E.P. Ippen, O.O. Olubuyide, J.S. Orcutt, M.J. Park, M.H. Perrott, M.A. Popović, P.T. Rakich, R.J. Ram, H.I. Smith, "Integrated optical components in silicon for high speed analog-to-digital conversion (Invited)," in Proceedings of the SPIE, Silicon Photonics II; vol. 6477-paper 22, Jan. 2007. (Photonics West 2007, San Jose, CA, Jan 24, 2007)

2. F.X. Kärtner, S. Akiyama, G. Barbastathis, T. Barwicz, H. Byun, D.T. Danielson, F. Gan, F. Grawert, C.W. Holzwarth, J.L. Hoyt, E.P. Ippen, M. Kim, L.C. Kimerling, J. Liu, J. Michel, O.O. Olubuyide, J.S. Orcutt, M. Park, M. Perrott, M.A. Popović, P.T. Rakich, R.J. Ram, H.I. Smith and M.R. Watts, "Electronic photonic integrated circuits for high speed, high resolution, analog to digital conversion (Invited)," in Proceedings of the SPIE, Silicon Photonics; vol. 6125, pp. 612503, Jan. 2006. (Photonics West 2006, San Jose, CA, Jan. 2006)

3. M.R. Watts, T. Barwicz, M.A. Popović, M. Qi, P.T. Rakich, L. Socci, E.P. Ippen, F.X. Kärtner, H.I. Smith and M. Romagnoli, "High-index-contrast microphotonics, from concept to implementation (Invited)," in Conference on Lasers and Electro-Optics (CLEO), OSA Technical Digest (Optical Society of America, Washington DC, May 21-26, 2006), paper CTuM3

4. T. Barwicz, M.A. Popović, P.T. Rakich, M.R. Watts, F.X. Kärtner, E.P. Ippen and H.I. Smith, "Fabrication control of the resonance frequencies of high-index-contrast microphotonic cavities (Invited)," in Proc. Integrated Photonics Research and Applications and Nanophotonics Topical Meeting (IPRA/Nano), Uncasville, Connecticut, April 2006, paper JWA3

5. R. Menon, H-Y Tsai, H. I. Smith, "Patterning and Imaging at the nanoscale with far-field optics via absorbance modulation," Technical Digest Photoninc metamaterials (2007)

6. H.I. Smith, T. Barwicz, C.W. Holzwarth, M.A. Popović, M.R. Watts, P.T. Rakich, M. Qi, R. Barreto, F.X. Kärtner and E.P. Ippen, "Strategies for fabricating strong-confinement microring filters and circuits (Invited)," scheduled for presentation at Optical Fiber Communication Conference 2007.

7. F.X. Kärtner, R. Amatya, G. Barbastathis, H. Byun, F. Gan, C.W. Holzwarth, J.L. Hoyt, E.P. Ippen, O.O. Olubuyide, J.S. Orcutt, M. Park, M. Perrott, M.A. Popović, P.T. Rakich, R.J. Ram, H.I. Smith, S. Takahashi, M. Geis, M.E. Grein, T.M. Lyszczarz, S.J. Spector and J.U. Yoon, "Silicon Electronic Photonic Integrated Circuits for High Speed Analog to Digital Conversion (Invited)," presented at the 3rd International Conference on Group IV Photonics (GFP 2006), Ottawa, Canada, Sep 14, 2006, paper ThC3

8. P.T. Rakich, M.A. Popović, M.R. Watts, T. Barwicz, H.I. Smith and E.P. Ippen, "Ultra-widely tunable photonic microcavities through evanescent field perturbation," in Conference on Lasers and Electro-Optics (CLEO), OSA Technical Digest (Optical Society of America, Washington DC, May 21-26, 2006), paper CTuM2

9. R. Amatya, C.W. Holzwarth, M.A. Popović, F. Gan, H.I. Smith, F. Kärtner and R.J. Ram, "Low Power Thermal Tuning of Second-order Microring Resonators," submitted to Conference on Lasers and Electro-Optics 2007.

10. T. Barwicz, C.W. Holzwarth, P.T. Rakich, M.A. Popović, E.P. Ippen, F.X. Kärtner and H.I. Smith, "Metallic-Contamination-Induced Optical Loss in Passive Silicon Microphotonics," submitted to Conference on Lasers and Electro-Optics 2007

Thesis:

1. Raul E. Barreto, "Fabrication of Optial –Mode Converters for Efficient Fiber-to-Silicon-Waveguide Couplers," MS Thesis, December 2006.

2. Corey Fucetola, "Resolution limits and process latitude of conformable contact nano-lithography," SM Thesis, February 2007.

3. J. M. LaPenta, " Real-time 3-d localization using radar and passive surface acoustic wave transponders," SM Thesis, August 2007.

4. H-Y. Tsai, "Absorbance Modulation Optical Lithography," SM Thesis, August 2007.